The formation of planets via pebble accretion

Thesis report

J. J. J. Liu

TUDelft

THE FORMATION OF PLANETS VIA PEBBLE ACCRETION

Thesis report

By

Jordi Jie Ju LIU

Student number: 4715586

to obtain the degree of Master of Science
at the Delft University of Technology

Thesis committee:

Dr. Wouter van der Wal,	Chairman, Technische Universiteit Delft
Dr. Stéphanie Cazaux,	Daily supervisor, Technische Universiteit Delft
Dr. Alessandra Menicucci,	Technische Universiteit Delft
Dr. Yamila Miguel,	Sterrewacht Leiden

PREFACE

Space has always intrigued me and being able to form planets for this thesis was such fulfilling to me. This project presented me lots of challenges, difficult times and but also moments of joy and victory, from which I was able to learn many things. For that I am very thankful my supervisor Stéphanie Cazaux who presented this project to me and was always enthusiastic and able to deliver me critical feedback and advice as my supervisor.

Jordi Jie Ju Liu
The Hague, April 2021

CONTENTS

SUMMARY

Planets form from micron sized particles existing in disks around stars. How does this process work? What are the steps taken to get gigantic planets when starting from tiny dust particles? These are the broad questions which are going to be explored in this thesis.

It is established that planets, planetesimals and centimetre sizes particles are present in the disk [1]. But what are the interactions between the larger and smaller bodies and is it possible for a growth model to exist where the the larger body can grow from these smaller particles? Unlike the established planetesimal accretion where growth is modelled via collisions between planetesimals, the growth in this case is called pebble accretion and involves the accretion of smaller pebbles onto larger bodies. This thesis aims to detail that process.

Planets are formed after several prior processes are completed. A Molecular Cloud is considered the first building block [2]. These are massive clouds of gas and dust and under physical processes such as gravity, turbulence, magnetic forces, gravitational collapse can occur. From the collapse, a system emerges consisting of a central star and a cloud of leftover material orbiting the central star. Over time, the material settles onto one single plane around the central star and is called the Protoplanetary disk (PPD). Within a PPD, physical processes such as accretion of dust, growth via collisions, radial drift take place. Planets are able to form as a result of these physical processes in the PPD.

Highlighting the settling process when forming a PPD, it is found that micron sized dust particles can grow during settling. As these particles travel towards the midplane, collisions and growth via accretion of dust, result in growth of the particle. The micron sized dust particle is able to grow into millimetre to centimetre sizes.

This is also where pebbles emerge as pebbles are determined by their Stokes numbers. A particle is considered a pebble when its Stokes number satisfies the following criterion: $10^{-3} < \tau_s < 1$ [−] [3]. The Stokes numbers of particles gives insight on the influence of the gas on the particle. Small particles with small Stokes numbers, smaller than 1 [−], are tightly coupled to the gas which means that the motions of the particle are influenced by the gas and the particle will align its motion with the gas. Large particles with large Stokes numbers, 1 [−] and larger, are decoupled from the gas. This means that the motion of the particle is independent from the gas.

With the pebbles on the midplane, an evolution of surface density of pebbles can be simulated via radial drift. As pebbles drift radially, the distribution of pebbles changes. Radial drift is dependent on the Stokes numbers of particles as well. particles with small Stokes numbers, are coupled to the gas but do not experience the radial pressure gradient [4]. This means that they will feel a net inwards force for radial drift. For large particles with Stokes numbers of larger than 1 [−], the motions are independent of the

gas. This means that gas will be experienced as drag which removes their angular momentum, causing them to spiral inwards.

Assuming a planet core to be present in the disk, it will be subjected to pebble accretion. Pebble accretion involves the accretion of pebbles onto larger bodies. The rate of accretion is dependent on the Stokes number of the pebble and the size of the planet. If the Stokes number is too small, the motion of the particle is dominated by the gas and the planet is not able to accrete the pebble.

In this thesis I will show that the formations of pebbles. Starting from settling micron sizes dust particles, and radially moving them inwards. Using these pebbles, a planet core is able to grow via pebble accretion. Planets are formed from the cores, varying in size depending on the radial distance.

1

INTRODUCTION

The key question about our universe is: 'How is it formed?'. This question hold lots of weight as the scale of our universe stretches into immense orders of magnitudes. From super massive black holes, to quasars, to neutron stars, to the cosmic microwave background. All of these fascinating phenomena have played a roll or are the result of our universe. Answering this key question is not a simple task and has to be done in a stepwise manner where the key question is broken down into smaller questions.

For this thesis, one of the smaller questions involves the formation of planets. There is a general consensus that accretion is the process leading into planet formation. However, observations show that centimetre and millimetre sized pebbles remain in the PPD for their entire lifetime [4]. For this reason, protoplanets and planetesimals coexist with these smaller grains and interactions between them are bound to present. This is in the form of pebble accretion where the larger body is able to gravitationally accrete the smaller pebbles. This is the foundation of pebble accretion and is detailed in this thesis. The objective is established to form planets using pebble accretion.

The main and sub-questions are give as:

How are planets formed by pebble accretion?

- *How do pebbles form from smaller particles?*

- *What is the effect of the turbulence and settling processes in the disk on the formation of pebbles?*

- *How do planets form from pebble accretion and can such a process lead to large planets?*

- *What masses do planets reach?*

In chapter 2, a basic understanding of planet formation is detailed. In this chapter, the processes are highlighted from a Molecular Cloud into planets. Then in chapter 3, the settling process is detailed. In this chapter, the settlement of particles onto the mid-plane is detailed which are the first steps in forming pebbles. Then, the results for the

1

simulations of the settlements are given in chapter 4 where pebbles are formed. Chapter 5 details the radial drift of the formed pebbles and particles before Chapter 6 details the growth of a planet core using the formed pebbles.

2

PLANET FORMATION

Planet formation is a process in which many steps are present. A basic explanation is given in this chapter, breaking down the planet formation in steps which are detailed in figure 2.1. The formation starts off with a Molecular Cloud (MC) and will undergo phase changes, structure changes, and evolves eventually into a star with accompanying planets. Figure 2.1 will act as a guideline in this chapter:
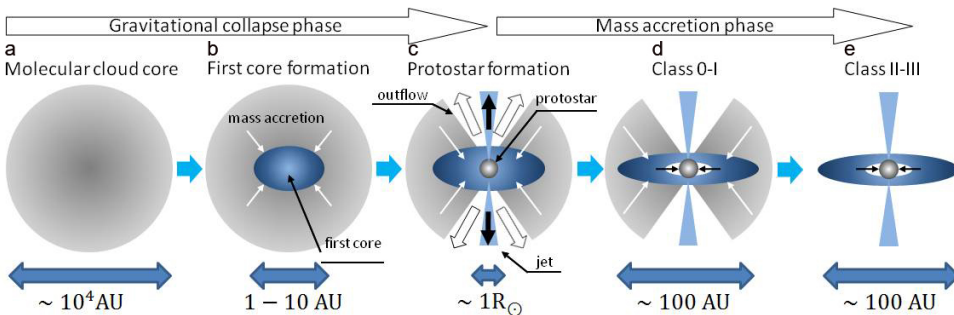
Figure 2.1: Visual showing the evolution steps from a MC to a disk with planets.[1]

2.1. FROM MOLECULAR CLOUD TO A STAR

In figure 2.1a, a Molecular Cloud (MC) core is is visualised, which are the initial building blocks for planet formation. MCs are massive clouds with sizes of 100 Parsecs to less than 1 Parsec, and with masses of 10^6 $M_\odot$ to less than $10^1 M_\odot$ [5]. These MCs are generally found near the galactic disk and consist of gas and dust particles. The MC is shielded from radiation from other sources, due to presence of dust. As a result of this, MC cores are cold with temperatures of about 10K. Lastly, MC are generally opaque and show up as dark sports in among the illuminated background.

---

[1]Taken from http://milkyway.sci.kagoshima-u.ac.jp/tsukamoto/study_en.html

The Eagle Nebula, catalogued as Messier 16 is a cluster which hosts many MCs. It is visualised in figure 2.2a, which is a photo taken by the Hubble Space telescope. Many MCs are present in the Eagle Nebula which are visible as darker sport in the figure. Within the Eagle nebula, a region is called the Pillars of creation and is visualised in figure 2.2b. This region houses the birth of many stars. In the figure 2.2b Evaporating Gaseous Globules (EGG) are observed. These are regions of gasses shielding the inner gas from ionisation from outer sources. The shielding can be observed as the outer gasses are ionised. This is visible on the top of the left hand pillar where the gasses are highlighted. This is detailed in figure 2.2c as well.

(a) Messier 16, Eagle nebula[2]

(b) Region in Messier 16, named the Pillars of Creation[3]

(c) Zoomed in figure of the left pillar[4]

Figure 2.2: Figures of Messier 16.

---

[4]Taken from https://www.eso.org/public/images/eso0926a/
[4]Taken from https://www.nasa.gov/image-feature/the-pillars-of-creation
[4]Taken from https://hubblesite.org/contents/media/images/1995/44/353-Image.html?news=true

2.1.1. COLLAPSE OF A MOLECULAR CLOUD

The second step highlighted in figure 2.1b is the formation of the core. When the MC core is dense enough, it will gravitationally collapse. Stable MC cores are in hydrostatic equilibrium; the gravitational attraction of the core is balanced by outward pressure forces, turbulent forces and magnetic forces. However, when the core is dense enough, the gravitational attraction of the dense core is able to overcome the resisting forces and gravitational collapse initiates. An important theory accompanying gravitational collapse is the Virial theorem, which relates the kinetic energy of a system with the potential energy (Ω). In case of a MC, the kinetic energy consist mostly of the thermal energy (U). The Virial theorem then states [6]:

$$2U + \Omega = 0 \; or \; U = -\frac{\Omega}{2} \tag{2.1}$$

For gravitational collapse to initiate, the potential energy needs to overcome the thermal or kinetic energy: $|-\Omega| > 2U$. The specific mass at which this occurs is called the Jeans mass. For an isothermal and homogeneous MC, the Jeans mass given as:

$$M_J = \left(\frac{5kT}{\mu m_H G}\right)^{\frac{3}{2}} \left(\frac{3}{4\pi\rho}\right)^{\frac{1}{2}} \tag{2.2}$$

Where k is the enclosed thermal energy, T is the temperature, μ is the molecular weight, m_H the molecular fraction of hydrogen, G the gravitational constant, of the material and and ρ the density.

When the Jeans mass is crossed, gravitational collapse occurs and the entire system will shrink. The whole envelope of material will move inwards towards the centre as the gravitational force is dominant. This results in a growing core, as material is accreted. More and more will get confined in the centre which results in more collisions and interactions between particles, this results in an increase of temperature and the thermal pressure. Eventually, this thermal pressure is large enough to withstand the gravitational force and balance is found again. Gravitational collapse stops and a system is formed with a proto-star in the centre and an envelope of gas and dust around the star.

2.2. FROM STAR TO PROTOPLANETARY DISK

Not all material from the MC ended in the central core of the MC to form the central star during gravitational collapse. The fall towards the core during collapse of material which were initially farther away will be stopped once gravitational collapse stops. If close to the core, the centripetal force is able to counteract the gravitational force of the central star and material will orbit the star forming a cloud. These are the building blocks of the Protoplanetary disk (PPD). Due to collisions between particles around the central star, perpendicular motions cease to exist and all material are focussed on a single plane: the orbital plane and forms a disk around that plane. This disk is often also referred as an accretion disk as the central star feeds on this disk. The net momentum of the disk results in rotation of the disk around the central star and together with accretion of the disk into the star, they form bi-polar outflow of some accreted mass. These outflows come in the form of collimated jets from the poles of the star. This way, more angular momentum is

2

dissipated from the system and the disk can slow down its spin. Eventually, the forming the PPD around the star.

2.3. FROM PROTOPLANETARY DISK TO PLANETS

Several processes take place within a PPD. In the inner region, accretion onto the central star takes place. However, in the outer regions, grains are able to coagulate due to small collisions among each other. This situation is visualised in figure 2.1d. As this process continues, larger bodies are formed, with their own gravitational field. These are the first steps of the formation of planets.

2.3.1. FORMATION OF THE PLANET CORE

There are several theories on the formation of planets. Two of the major ones are detailed in this section.

Planetesimal accretion   The motion of particles in the PPD are dominated by the gas in the PPD; the particles are coupled to the gas. Micron sized grains up until centimetre sized pebbles, their movements are dominated by the motions of the gas. Collisions among these grains take place during settlement towards the midplane, allowing for grains to grow into centimetre sized pebbles. The formation of larger planetesimals is not fully understood yet [2] as particle growth beyond centimetre sizes is inefficient [7]. However, the most economical hypothesis states that this process continues until planetesimals are formed [8].

Cores formed from accretion of solid planetesimals are able to decouple from the gas and are able to travel along their own Keplerian trajectories [9]. This results in these bodies experiencing the gas as a drag, as the gas travels in with sub-Keplerian velocities. Due to the experienced drag, the larger bodies lose some of their angular momentum resulting in radial drift. The radial drift allows for the larger bodies to sweep material on its radial voyage and grow even more.

Pebble accretion   Pebble accretion is a concept of planet formation which involves the accretion of smaller pebbles onto larger masses. [3]. This concept is a major detail in this thesis and more depth will be given into pebble accretion in chapter 6. The interaction between the smaller pebbles and larger bodies depends on the friction time of pebbles. The friction time is defined as:

$$t_f = \frac{\rho_p}{\rho_g} \frac{a}{\bar{v}} \tag{2.3}$$

Where ρ_p is the density of the particle, ρ_g is the gas density, a is the radius of the pebble and $\bar{v}$ is the mean thermal velocity. The friction time defines the timescale at which the pebble with a relative velocity will align itself with the local gas again. If coupled to the gas, the friction time is short and if less coupled to the gas, the friction time is longer. If decoupled, the particle is able to follow its own trajectory. Within pebble accretion, the accretion of these pebbles is dependent on the time to accrete the pebble relative to the friction timescale of the pebble. In figure 2.3, interactions between larger body and pebble are visualised .
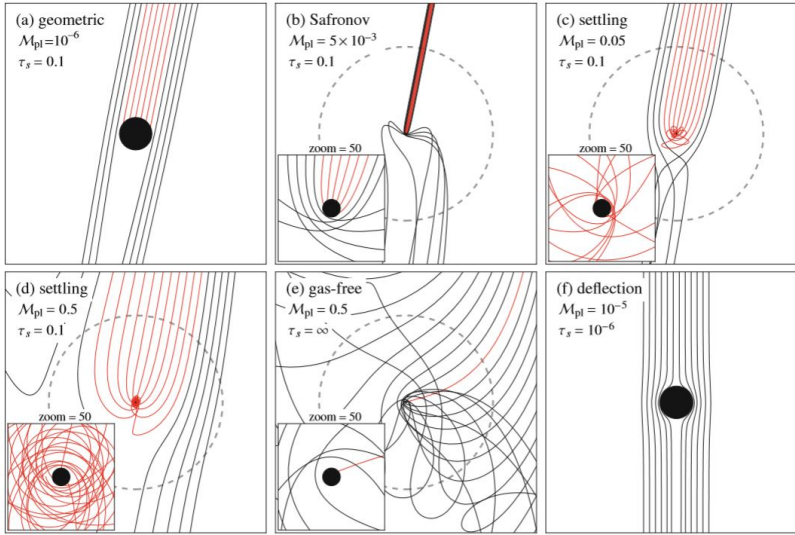
Figure 2.3: Several pebble accretion encounters are visualised in this figure. In each figure, the *dark circle* represents the planet and the *dashed circle* represents the Hill Radius of that planet. Pebbles enter from the top and the planet mass is given by M_{pl}. Trajectories of the pebbles are given by the *red lines*. Figures *c and d* qualify as pebble accretion while figures *a, b and e* qualify as ballistic. In figure *f*, the particles are so small that they follow gas. Taken from Ormel [3]

In figure 2.3a, the mass of the planet is not large enough. The time to accrete the pebbles (black lines) is larger than the friction timescale of the pebbles. In figure 2.3b, the mass of the planet is larger and is able to perturb the trajectories of the pebbles passing the planets Hill sphere. However, the time required to accrete is still larger than the friction timescale, and the pebbles are only scattered. Figure 2.3c is where the mass of the planet is large enough and the time of accretion is smaller than the friction timescale. The time to accrete the pebble is shorter than the pebble can align itself with the gas and the pebble is accreted. Figure 2.3d shows an even larger planet and even more pebbles are accreted. Figure 2.3e shows a situation where there is no gas. As there is no gas, the pebbles move along their own trajectories and the planet is not able to accrete the pebbles. Figure 2.3f visualises a case where the gas density is large. Pebbles are very coupled to the gas and the planet is not able to accrete the pebbles.

2.4. MIGRATION

Planets in the protoplanetary disk are subject to migration. This is caused by tidal interactions between the planet and the gaseous disk as angular momentum is interchanged [10]. The net angular momentum for the planet is not zero, and results in the planet migrating radially. This occurs when the gas in the disk is able to apple differential torques on the planet. The types of migration and the physics behind them is explained in this section.

2.4.1. TYPE-I MIGRATION

Bodies with Earth masses in the PPD are candidates to experience type-I migration [11]. These bodies are not large enough to clear a gap in the surroundings of the disk and when this is the case, excitations from Lindblad resonances drive spiral density waves in the disk. These result in torques on the planet, which either increases the angular momentum or decreases the angular momentum. This is visualised in figure 2.4. A planet is positioned in the disk and undergoes type-I migration. The spiral density waves are visible as the higher density areas inwards the disk from the planet, and also the higher density area outwards from the planet. The inner wave adds angular momentum while the outer wave decreases the angular momentum of the planet and as the outer wave is larger, the planet will experience a net loss in angular momentum. This causes the planet to radially migrate inwards.

Figure 2.4: Figure of the spiral density waves. The inner wave applies positive torques on the planet and the outer wave applies negative torque on the planet. The planet will experience a net negative torque as the outer wave outmatches the inner wave. This results in inward drift of the planet (F. Masset)[5]
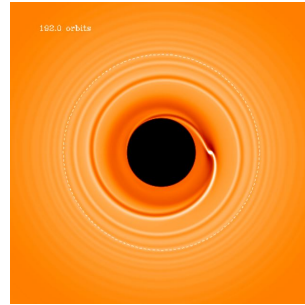
2.4.2. TYPE-II MIGRATION

Type-II migration is applicable for larger planets which are able to create a local gap in the gaseous disk. when this happens, the radial movement of the planet becomes coupled to evolution of the PPD. The central continues its feeding, and accretion takes place which results in the gas slowly moving towards the central star. The radial movement of the giant planet is now coupled to this inwards movement. Figure 2.5 visualises the large planet, and the gap it has created. In such a scenario, the planet slowly moves along with the surrounding gas around the gap.

Figure 2.5: A figure of a planet and gap created by the planet.[6]

---

[6] https://www.fis.unam.mx/~masset/moviesmpegs.html
[6] https://www.fis.unam.mx/~masset/moviesmpegs.html
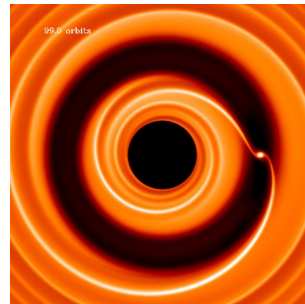
3

PARTICLE GROWTH

When the nebula has formed from the MC, it starts cooling and dust grains will condense. The growth of these dust grains stands as one of the first steps of planet formation [2]. The physics of the growth involve collisions between these particles, which allows for sticking and results in larger particles. The collisions between these particles are caused by relative motions between particles which are induced by different physical processes. The relative velocities induced for the smallest particles are caused by Brownian motion [12]. This motion provides velocities of mm/s to cm/s for the particles to grow and is explored in section 3.1. Then, in section 3.2, the growth as a result of settling is explored which is caused by the settlement of particles. As particles are moving downwards, the velocity relative to the dust and other particles allows for growth as well and is detailed.

From this point, a particle is referred as a family of particles. A family of particles is a group of particles which originate from a single height and are the objects which grow. The family will have a number density of particles, each with the same radius and mass. As they settle downwards, their position above the midplane changes, but are referenced by their original position. This means that a particle (family) $4h$ originates from $z = 4h$ above the midplane.

3.1. BROWNIAN COAGULATION

Brownian growth or coagulation is the result of growth due to random velocities between particles. This motion is caused by the thermal motion of the gas . Smaller particles are more affected by this motion due to the fact that gas and particles motions are coupled. In this section, this effect is taken into consideration as the source for growth of particles.

3.1.1. BROWNIAN MOTION

Brownian motion is the random motion of particles suspended in a gas. A particle in a gas will encounter collisions with the gas particles in its environment which will cause momentum exchange, changing the course of particles trajectory. Many collisions between the gas particles and the particle, result in arbitrary motions. These motions are

dependent on the temperature of the gas, the dimensions of the particle, initial motion of the particle, temperature and velocity of the gas particle.

The relative velocity of a particle 1 with respect to a particle 2 is given as [12]:

$$v_{Brownian} = \sqrt{\frac{8 k_b T (m_1 + m_2)}{\pi m_1 m_2}} \tag{3.1}$$

Where k_b is the Boltzman constant, T is the temperature of the gas, m_1 is the mass of the particle and m_2 is the mass of particle colliding with the growing particle.

3.1.2. COAGULATION DUE TO BROWNIAN MOTION

The growth of a particle family due to Brownian motion is estimated by the following equation [13]:

$$\frac{dm}{dt} = \pi a^2 \cdot |v_{Brownian}| \cdot \rho_{dust} \tag{3.2}$$

Where a is the radius of the particle, $v_{Brownian}$ the velocity of the relative Brownian motion with respect to the gas and ρ_{dust} is the dust density. This equation explains the growth of a particle of radius a by sweeping the dust particles with a relative velocity $v_{Brownian}$.

The dust density ρ_d is retrieved from gas-to-dust ratio where:

$$\rho_{dust} = f \cdot \rho_{gas} \tag{3.3}$$

Where f is set to be 0.01 [14]. The gas density for the particular column at 1 AU is a function of the height above the midplane following an exponential function. Gas is thinner at higher altitudes, and is thickest at the lowest altitude, on the midplane. This exponential function for the gas density is given as [4]:

$$\rho_{gas}(z) = \frac{\Sigma}{h\sqrt{2\pi}} e^{-z^2/2h^2} \tag{3.4}$$

Where z is the height above the midplane, h is the pressure scaleheight and Σ is the surface density at a specific radius. This surface density is modelled after:

$$\Sigma = \beta \left(\frac{r}{AU}\right)^{-1} \tag{3.5}$$

Where $\beta = 500 \frac{grams}{cm^2}$. Assuming that m_2 in equation 3.1 consists of only 1 micron sized dust particles, the growth of 1 micron-sized particles as a function of time is determined and reported in figure 3.1. This figure represents the growth particles at different heights above the midplane. The result shows that growth of particles is dependent on the height above the midplane. Particles at higher altitudes grow very little, while particles at lower altitudes grow more. This is evident in figure 3.1 where the green line represents the growth of the particle at $z = 0$, that grows into the largest particle.

The height dependence of the growth is the result of the dust density ρ_{dust} in equation 3.2. As both the dust and the gas density are a function of the height above the midplane as seen in equation 3.4. This phenomenon holds true as more Brownian growth takes place in regions with higher density. In denser regions, particle collisions are much more frequently than in less dense regions as more particles are confined in the same space. With more collisions particles are able to grow much more.
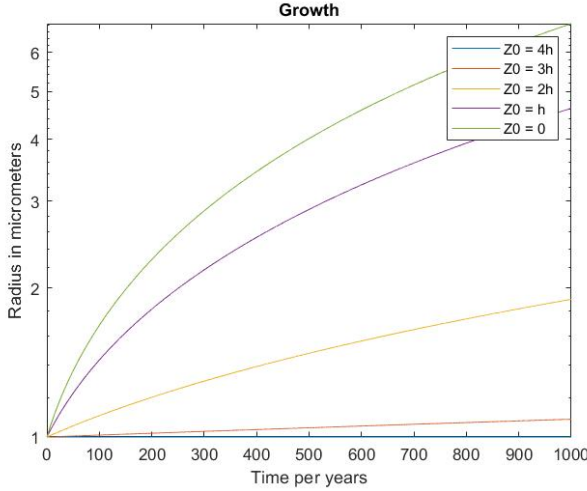
Figure 3.1: Growth of the radius of particles as a result of Brownian motion. Their distance from the central star is 1 AU, with a local scaleheight of $3 \cdot 10^{11}$ $[cm]$ and particle density of 3 $\left[\frac{gram}{cm^3}\right]$ Each line represents a particle different heights above the midplane and over time, the particle grow in size.

3.1.3. DUST DECREASE

In the precious subsection, the growth of the dust particles into particles was based on the assumption that the dust density ρ_{dust} would remain constant while only $v_{Brownian}$ and the radius a would change in equation 3.2. However, this is not the case as dust is used for the growth of particles and the dust should decrease. Initially, the dust density is assumed to be a fraction of the gas density 3.3.

The orange line in figure 3.2 represents the dust density which consists of only 1 micron sized dust particles that can grow into larger sized particles. Quantifying the amount of dust present in the dust density, the number density is calculated:

$$n = \frac{\rho_{dust}}{m_{dust}} \left[\frac{1}{cm^3}\right] \tag{3.6}$$

Where m_{dust} is the mass of 1 micron sized particles. With the number density, the decrease in dust density due to growth the particles can be calculated:

$$d\rho_{dust} = dm \cdot n \left[\frac{grams}{cm^3}\right] \tag{3.7}$$

Where dm is calculated in equation 3.2 and n is calculated in equation 3.6. Equation 3.7 represents the decrease in dust density due to particles growing and taking away some mass from the dust reservoir. The evolution of the dust density with time is the calculated, and is shown in figure 3.3.

From figure 3.3, it can be observed that the dust density decreases over time in the lower regions near the midplane. The upper regions at $4h$, the dust decreases little. This is due to the Brownian growth, where growth is more prominent in the lower regions and less in the upper regions.
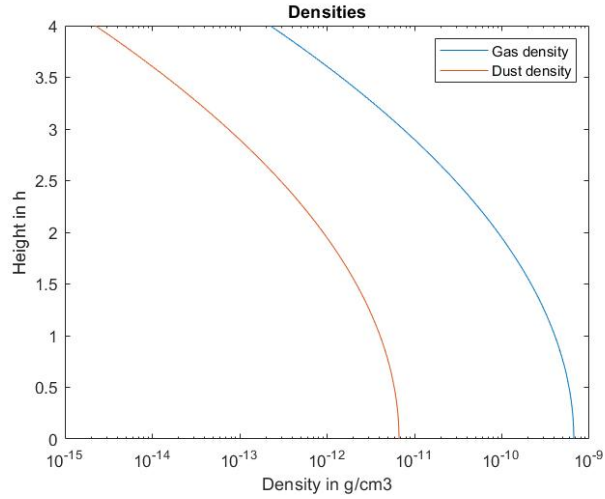
Figure 3.2: The gas and dust densities at a distance of 1 AU from the central star assuming a gas surface density $\Sigma = 3 \left[\frac{gram}{cm^3} \right]$, and local scaleheight of $h = 3 \cdot 10^{11} \ [cm]$.
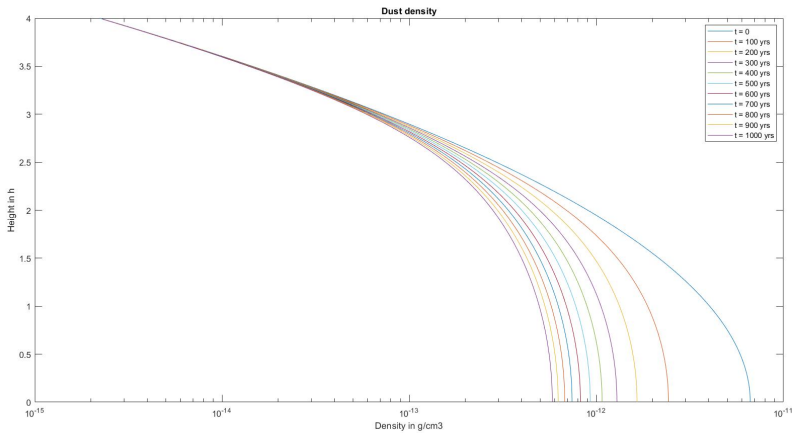
Figure 3.3: The dust density over years. The blue line represents the initial dust density and it can be observed that the dust decreases over the years as particles are growing, taking away the dust particles.

Paired with this new decrease in dust, the new growth figure of the particles is given in figure 3.4. In figure 3.4, the growth of the particles are given taking into account the decreasing dust density and compared to figure 3.1, the particle does not grow as much as previously when the dust reservoir was constant. This is due to the decrease in dust, as there is less dust to gain mass from.

As it can be seen, particles do not grow substantially over a period of 1000 years according to figure 3.4. When dust decreases, the growth of the particles decreases and
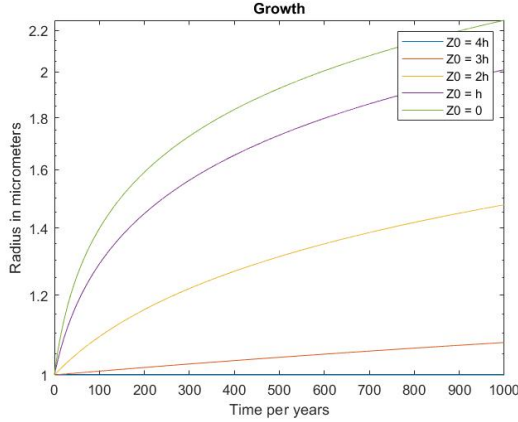
Figure 3.4: Growth of particles due to Brownian motion. It can be seen that the particles grow less when the dust is evolving. As the dust is evolving, it will decrease which leaves less mass for the particles to grow from. This results in smaller particles than the situation where a constant density is considered

eventually the growth of the particles will stagnate.

3.2. SETTLING AND COAGULATION

Small particles above the midplane experience forces such as the gravitational attraction from the star, which causes them to move towards the midplane. This downwards movement is called settling and is the process which causes gas and dust to locate itself near the midplane disks around a star.

3.2.1. DRAG PHYSICS

When a particle is moving, through a medium, it will experience different drag forces depending on the mean free path λ of the medium, and the radius a of the particle. Based on these parameters, the drag forces are written for different mediums [15]:

1 For the fluid regime:

$$F_D = \frac{1}{2} C_D \pi a^2 \rho v^2 \tag{3.8}$$

2 For the particle regime:

$$F_D \simeq \frac{4\pi}{3} \rho a^2 v \bar{v} \tag{3.9}$$

Where v is the velocity of the particle with respect to the medium, ρ is the density of the medium and $\bar{v}$ is the thermal velocity of the medium. Equation 3.8 is only valid for particles which are moving through a fluid, and equation 3.9 is only valid for particles which are moving through a regime of gas.

Moving through the nebula, particles will feel the gas acting as a drag force. When feeling this drag force from the gas, the relative movement of the particle with respect to the gas will decreases until the particle is fully 'coupled' to the gas. In this state, the

movement of the particle is fully dominated by the gas. The time required for a particle with a relative velocity to lose all of its velocity is given as the *friction time scale*:

$$t_{fric} = \frac{mv}{|F_D|} = \frac{\rho_p}{\rho_{gas}} \frac{a}{\bar{v}} \tag{3.10}$$

Where m is the mass of the particle, ρ_p is the density of the particle and ρ_{gas} is the density of the gas.

The Stokes number is dimensionless number which is used for the characterisation of particles in a medium and is defined as [3]:

$$\tau = t_{fric}\Omega \tag{3.11}$$

Where Ω is the orbital frequency. A particle with low Stokes numbers is tightly coupled to the medium it is moving through. In the case of particles in the PPD, the particles are tightly coupled to the gas. Particles with large stokes number are decoupled from the gas and move along their own trajectory and feel the gas as drag. Generally, particles which are tightly coupled to the gas have low Stokes numbers, lower than 1 and decoupled particles have Stoke numbers larger than 1. The extend of how much a particle is coupled to the gas in a PPD, is dependent on several parameters. These are explained below:

- **The gas density**: it can be observed that the gas density is present in the friction time, equation 3.10. For a denser gas cloud, a particle will feel more gas drag which decreases the friction time. A particle will then be more easily coupled to the gas and have lower Stokes numbers;

- **The mass of the particle**: a particle with larger mass requires more gas drag to slow down than particles with smaller masses. This increases the friction time and thus also the Stokes number. A particle with large mass has a higher Stokes number than particles with low mass;

- **The radius of the particle**: a particle with a large cross section will feel more drag than particles with smaller cross sections. So, larger particles slow down more easily than smaller particles (assuming that the masses are equal). A particle with a larger cross section has a lower Stokes number than a particle with a smaller frontal area.

3.2.2. SETTLING MOTION

Particles formed at higher elevations from the midplane of a PPD will eventually end up in the midplane. Two forces are dominating the motion towards the midplane. These are the vertical component of the gravitational force exerted by the central star and the gas drag experienced by the particle and are written as [4]

$$F_{grav} = m\Omega^2 z \tag{3.12}$$

$$F_d = \frac{4}{3}\pi a^3 \bar{v}\rho v \tag{3.13}$$

Where m is the mass of the particle, a is the radius of the particle, Ω is the orbital frequency , $\bar{v}$ is the local thermal velocity, v is the velocity of the particle and z is the

height above the midplane. Combining these two equations and solving for v leads to the terminal velocity of the falling particle. This terminal velocity is quickly attained by the falling particle as the particle is still small and closely coupled to the gas. This velocity is called the settling velocity:

$$v_{settle} = \left(\frac{\Omega^2}{\bar{v}}\right) \frac{\rho_p}{\rho_g} az \tag{3.14}$$

Where ρ_p is the density of the particle and ρ_g is the gas density as described in equation 3.4.

When studying the settling velocity in equation 3.14, one can determine that it is a function of the radius of the particle and the height, and inversely dependent on the gas density. So, a particle will settle faster at higher altitudes and with larger sizes. This is visualised in figures 3.5:
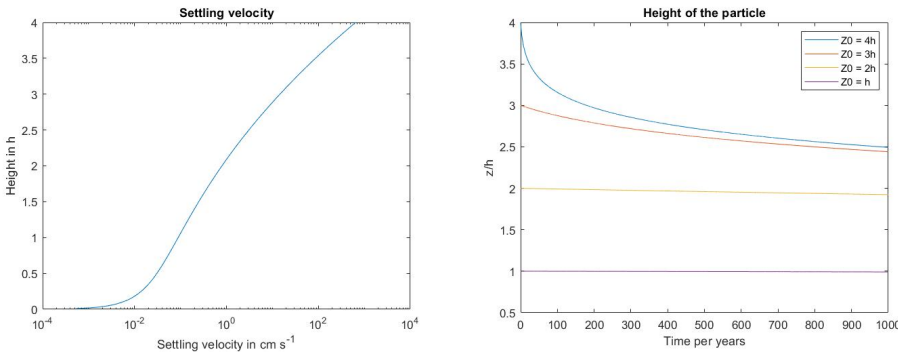
Figure 3.5: Left) The settling velocity over height. Right) the heights of particles over time where each line represents a particle falling from a specific height. This calculation performed at a radius of 1 AU and starting from a height of $4h$ with a particle radius of 1 μm and density of 3 $gram \cdot cm^{-3}$. It can be observed from the left hand figure that the settling velocity is large at higher altitudes and is small at lower altitudes. This is due to the dependence of the height itself and on the inverse dependence of gas density, which increases at lower altitudes.

It can be seen in figure 3.5 that the velocity is calculated to be about 0.1 centimetre per second at $1h$. At a radius of 1 AU from the central star, this translates to a settling time of about 2×10^5 $years$, which is too long as this settling process is expected to proceed rapidly compared to the lifetime of a PPD of a few million years [16].

3.2.3. COAGULATION DUE TO SETTLING

During settling, the particle will encounter other particles in the gas and dust and due to these encounters, the particle will grow as a result of coagulation. The mass growth can be written similarly as in equation 3.2, a function of the cross section of the particle, the local velocity, which in this case is the settling velocity, and the dust density [4]

$$\frac{dm}{dt} = \pi a^2 \cdot |v_{settle}| \cdot \rho_{dust} \tag{3.15}$$

Where the dust density is calculated according to equation 3.3. Filling in the settling velocity described in equation 3.14 and the dust density in equation 3.3 into equation

3.19:

$$\frac{dm}{dt} = \frac{3}{4} \frac{mf\Omega^2}{\bar{v}} z \qquad (3.16)$$

This equation 3.16 describes the change in mass of a settling particle where dust density is calculated using a dust-to-gas ratio from the gas density. When solving for the vertical height of the particle, the settling velocity is taken:

$$\frac{dz}{dt} = -\left(\frac{\Omega^2}{\bar{v}}\right) \frac{\rho_d}{\rho_g} az \qquad (3.17)$$

These two equations 3.16 and 3.17 describe the movement and growth of a particle moving from an altitude downwards, towards the midplane. Its movement is dominated by the vertical component of the gravitational force of the central star and the gas drag. The resulting growth and vertical movement are given in figure 3.6:
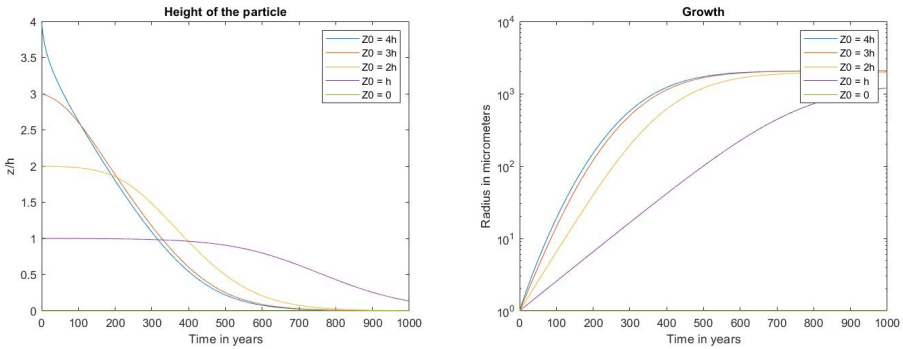
Figure 3.6: Left) The height of particles above the midplane where each line represents a particle starting from a specific height. Right) The growth of particles starting from different heights above the midplane. Each line represents a particle starting from a different height above the midplane.

Figure 3.6 shows the settling of the particle on the left hand panel, and the growth of the particle on the right hand panel. The horizontal axis represents the time. The left hand panel visualises the height over time, and the right hand panel represents the sizes of the particles over time. Each line represents a particle family settling from different initial heights. The following points can be observed from figure 3.6:

- The settling velocity is large at higher altitudes above the midplane and small near the midplane. Particles in higher regions move very rapidly while particles at lower altitudes move very slow;

- Growth is dependent on the settling velocity. This results in large growth when the settling velocity is large, and little growth when the settling velocity is small. It can be seen that the particle starting from $4h$ grows fastest when falling most rapidly downwards and slows down when the settling velocity decreases near $t = 400$ years. After 1000 years, millimetre sized particles are formed.

3.2.4. DUST DECREASE

Just as in section 3.1.3, the dust density decreases when particles are growing and this decrease of the dust reservoir applies for settling as well. The behaviour of how the dust will decrease depends on the position of the particles and the amount of growth. As seen in figure 3.6, particles high up grow fast and particles in the lower regions grow much slower.

In section 3.1.3, the amount of particles in the dust was calculated to be:

$$n = \frac{\rho_{dust}}{m} \left[\frac{1}{cm^3} \right] \tag{3.18}$$

Where in this case the ρ_{dust} is the local dust density dependent on the height and m is the particle which grows from taking away dust from the local dust density. The rate at which the dust decreases is given as:

$$d\rho_{dust} = n \cdot dm \left[\frac{grams}{cm^3} \right]$$

Where dm is the growth of a single particle given in equation 3.19. In this situation, the decrease in dust is dependent on the following:

- The size of the growing particle. It is established that larger particles sweep more mass based on equation 3.19;

- The height of the particle influences the settling velocity. The settling velocity is higher at higher altitudes, and results in larger particle growth and thus, also results in larger dust decrease.

With the decrease of dust taken into account, the figure 3.7 is plotted which visualised the decrease of dust density over time due to settling. It can be seen that the 'middle' part at around $3h$ to $0.5h$ severely decreases in dust density while the most upper regions and the lower regions remain constant. These have the following reasons:

- The upper region remains constant because most particles which grow settle and most particles have already left the upper regions. This can be seen in figure 3.8. The particles in the upper regions grow fastest, but settle fastest as well. This results in the fact that there are no more particles left in the upper regions and no more growth takes place; the dust remains constant;

- The inner region decreases due to the fact that both particles which start off in that region grow and take away mass from the dust, and particles coming from the upper regions arrive here and take away mass. This can also be seen in figure 3.8 where majority of the particles ($4h$, $3h$ and $2h$) are present in the middle region;

- The lower regions remains constant as a result of the low settling velocity in the lower regions. As the growth is dependent on the settling velocity, little growth will take place in the lower regions as the settling velocity of the particles is very low. This in term, results in no decrease in dust density and is also visible in figure 3.8 where the particles are not able to reach the midplane.
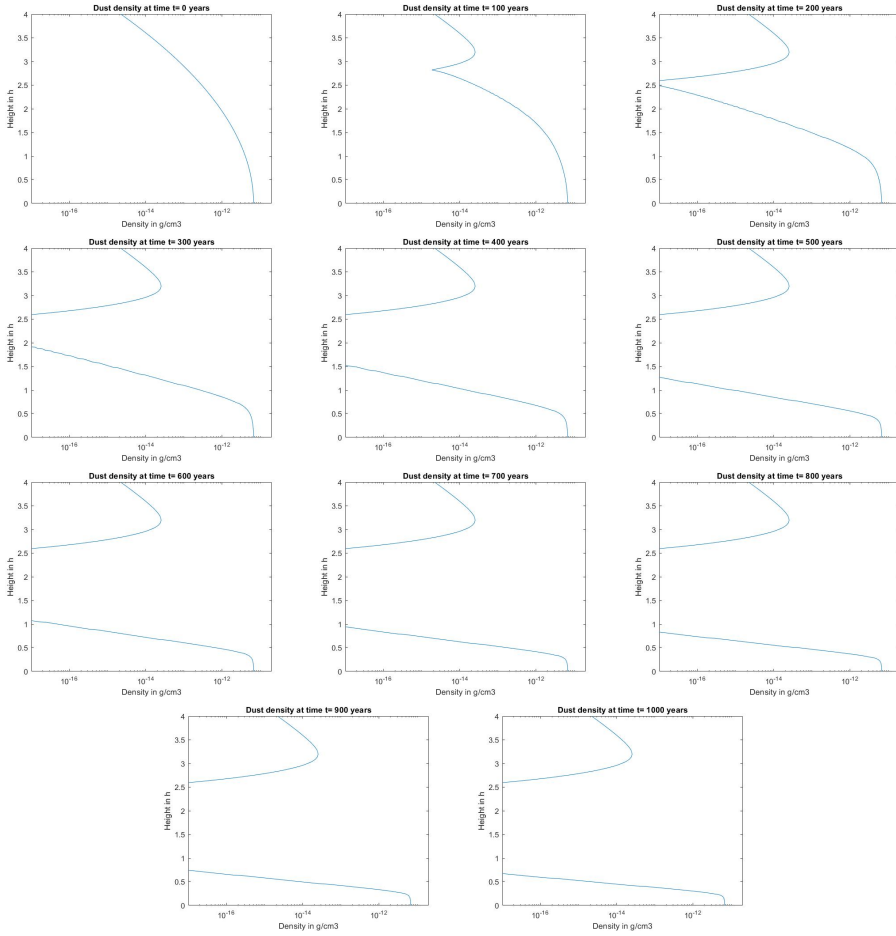
Figure 3.7: The dust density over time. Each figure represents the dust density at a specific time. The upper left figure represents the time at $t = 0$ years and the lower right represents the time $t = 1000$ years.

Accompanied with the new decrease in dust, the growth and height figures of the particles is given in figure 3.8. In this figure, it can be seen that particles do not grow larger than 7 microns, and settling eventually stagnates. The main reason why this occurs is due to the decrease in dust density, as it plays an important role:

- Particles grown into a few micron sizes due to the decrease of dust density. As stated in equation 3.19, the growth is dependent on the dust density. As most particles settle downwards, the regions at $3h$ to $1h$ are flooded with particles, each growing by taking away dust. The dust decreases drastically which also drastically decreases the growth of the particles themselves;

- The stagnation of settling is indirectly the result of the decrease in dust density. As the dust density decreases, particles have less mass to grow from. However, the
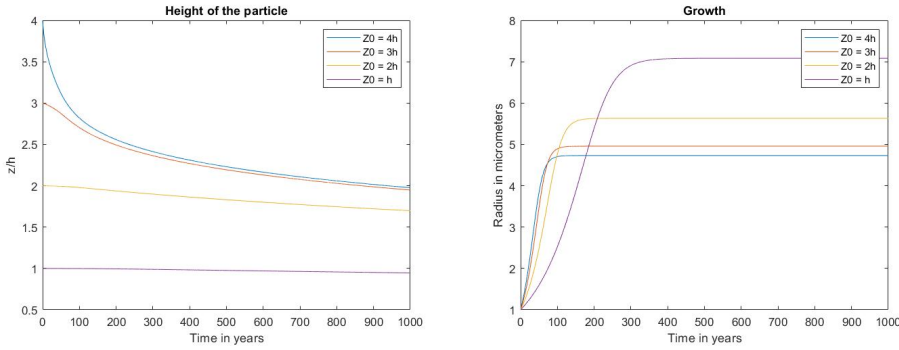
Figure 3.8: Left) The height of particles above the midplane where each line represents a particle starting from a specific height. Right) The growth of particles starting from different heights above the midplane. Each line represents a particle starting from a different height above the midplane.

settling velocity is dependent on the sizes of the particles as seen in equation 3.14. When particles do not grow into large enough sizes, particles will seize to settle and stagnate.

3.3. GROWTH VIA COLLISIONS

In the previous sections, it was described how particles were able to grow via sweeping the dust density. However, particles are also able to grow via collisions with other particles. When two particles collide, growth occurs where the larger one gains mass from the smaller one. The growth of a larger particle a colliding with smaller particle b is then described as:

$$\frac{dm_a}{dt} = \pi a_a^2 \cdot |\Delta v| \cdot \rho_b \tag{3.19}$$

Where Δv is the difference in settling velocity between larger particle a and smaller particle b, and ρ_b is the particle density of the smaller particle family b. The density increase for particle family a is equal to the density decrease for particle b and is then described as:

$$d\rho = n_a \cdot dm_a \tag{3.20}$$

Where n_a is the number density of particle family a and dm_a is the mass gain of a single particle a. The change in density described in equation 3.20 is the increase in density for particle family a and the decrease in density for particle family b. Results for this model will be shown in the next chapter.

4

FORMATION OF PEBBLES

As described in chapter 2, pebble accretion is a growth model for the formation of planets from pebbles. It involves the the accretion of small particles with negligible mass onto larger bodies. Gas drag and gravity play large roles in pebble accretion. There are two definitions for aerodynamically small pebbles. One of them is given by M. Lambrechts et al. [16] and another one given by C. Ormel [3]. Both of these definitions are explored in this chapter. In this chapter, the results from the previous chapters are used to conclude whether or not pebbles are formed from settling and coagulations.

Lastly, two additional phenomena are taken into consideration when growing the particles: gas decay and turbulent motions. Incorporating these phenomena yields different results and is also detailed in this chapter.

4.1. THE DEFINITION OF PEBBLES

4.1.1. DEFINITION BY C. ORMEL

According to C. Ormel [3] pebbles are particles which meet a certain criterion: *"Pebbles are particles which have Stokes numbers of* $0.001 < \tau < 1$ *"* [3]. The Stokes number has effects on the accretion of pebbles by planet cores. Pebbles need to be aerodynamically small, for the core to accrete pebbles. For Stokes numbers which are even smaller than 10^{-3}, the trajectory of pebbles would be dominated by the gas and if the Stokes number would be too large, the pebbles would follow a ballistic trajectory around the core.

4.1.2. DEFINITION BY M. LAMBRECHTS

For the calculations in [16], a pebble was defined as any particle with a radius of larger than $1\,mm$. With this specific radius, the pebbles have radial drift motions and pebbles are able to drift and act as a source of material for planetesimals to grow from. This implies that there will be pebble accretion is possible as there is a constant inflow of pebbles from outer radial distances.

4.2. RESULTS

This subsection details the results from the previous chapters where the Brownian growth, settling and coagulation, and collisions are combined. Three simulations are performed, one with standard settling and coagulation, one combined with a gas decay model, and one combined with turbulence. Results are shown for three radial distances from the central star: 1AU, 10AU and 50AU.

4.2.1. RESULTS FOR THE STANDARD MODEL WITH SETTLING AND COAGULATION

PARTICLE GROWTH

Figure 4.1 shows the evolution of the particles. Three evolutions are visualised, the first row is performed at $r = 1$AU with a simulation time of 1000 years, the second row at $r = 10$AU and the third row is performed at $r = 50$AU, which are both performed with a simulation time of 10000 years. The left column of figure 4.1 visualises the settling of the particles and the right column visualises their growth while settling. Each line in the figures represents a particle settling onto the midplane, and each of them start from a different height above the midplane, which are indicated by the different colours.

The largest particles are formed at $r = 1$AU where particles from an altitude $4h$ grow into particles of about sub-250 microns. Other particles which start from lower altitudes grow little compared to the one from 4h and settle very slowly, as seen in figure 4.1 where these particle remain in near their original starting position above the midplane.

For particles farther away at $r = 10$AU, it can be seen that the growth is just as prominent as at $r = 1$AU. However, the growth initiates later as can be seen in figure 4.1d where the growth increases rapidly after about 2000 years. The settling of the particles is also slower than the particles from $r = 1$AU. At a time of 2000 years, the particle from $4h$ would only have settled onto about $2h$. The 'middle region' is the region where most particles are present due to the drag experienced. This results in many collisions and encounters, and therefore, the largest particles would experience more growth and settling after this growth. This is the reason for the growth which initiates later.

Lastly, slow settling and little growth is evident from the particles at $r = 50$AU. Settling for particles which originate from higher regions at 4h stagnated at about a height of $3h$ and is barely visible for the particles originating from lower altitudes, for instance at 1h. Growth is also barely visible as the particles only grow by fractions of microns.

The following points can be observed from the figures:

- The Brownian growth is small compared to the settling growth and is only present in the lowest layers of the disk, on the midplane. This is evident from the growth of the particles on the midplane in figure 4.1. Only the particles at $z = 0$ grow via Brownian growth as their growth is linear unlike the settling which is dependent on the settling velocity. The Brownian velocity and settling velocity are visualised in 4.2;

- The growth of the particles are strongly dependent on the collisions. In figure 4.1a and b, particle family $4h$ (blue line) settles rapidly within the first 200 years. At 200 years, the settling slows down, before decreasing rapidly again. The initial rapid

(a) Settling at $r = 1$AU

(b) Growth at $r = 1$AU

4

(c) Settling at $r = 10$AU

(d) Growth at $r = 10$AU

(e) Settling at $r = 50$AU

(f) Growth at $r = 50$AU
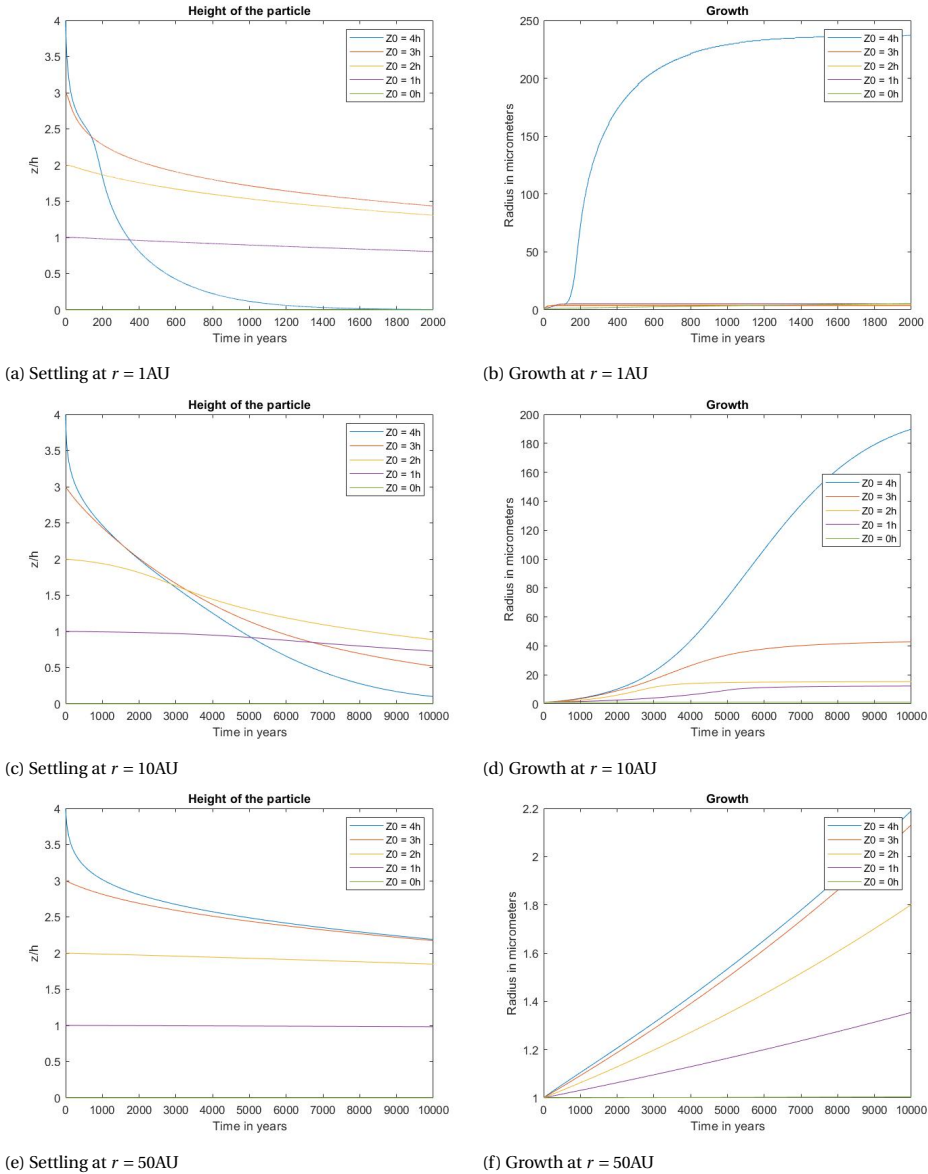
Figure 4.1: Each row represents results from a different radial distance from central star. The upper row stands for 1AU, second row for 10AU, the third row for 50AU. left) the settling of particles towards the midplane. Each line represents a particle starting from a height. Right) The growth of the particles when settling onto the midplane. Each line represents one particle starting from a height above the midplane.

decrease is due to the high altitude, as settling is larger at higher altitudes. After reaching lower altitudes at 200 years, the gas drag kicks in and the vertical movement slows down. However, once reaching this region, encounters between parti-
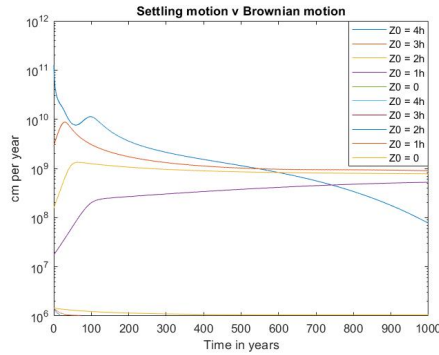
Figure 4.2: The settling velocity versus the Brownian velocity. The lines in the middle of the figure represent the settling velocity of the particles, and the lines at the bottom of the figure are the Brownian velocity of the particles. It can be seen that the settling velocity of nearly all particles are larger than the Brownian velocity.

cles occur as there are more particles clumped in this region due to the gas drag. Particle family $4h$ is able to grow from from those particles settle again;

- The particle families which start from lower altitudes, about $2.5h$ to $0.5h$ do not grow much as they are already in regions where the gas drag is the dominant vertical force. This does not allow for settling and thus, also no or little growth. One point to note is that these particles do not grow via Brownian growth even when their settling is little. This is due to the fact that their relative Brownian motion with respect to the dust is even smaller than their small settling velocity. Which means that they still settle and grow via settling, only very slowly. Their main purpose in this case is to facilitate the growth of larger particles which are passing onto the midplane.

Dust evolution

The dust evolution for each radii is given in figure 4.3.

Figure 4.3 visualises the evolution of the dust density when particles are settling as shown in figure 4.1. In the figure representing $r = 1\text{AU}$, it can be seen that the dust density decreases over time. Especially in the 'middle' region between heights $3h$ and $0.5h$. It can be seen that, compared to the initial dust density at $t = 0$, the dust density decreases within this middle regions while the upper region above $3h$ and near the midplane below $0.5h$, the remains mostly constant.

The decrease in dust density in the middle region is explained by the settling of the particles from figure 4.1. As most particles are settling, they will gradually slow down when reaching lower regions. A lot of particles from upper regions slow down in the middle regions where they grow by collecting dust. This is then seen as the large decrease in dust density in figure 4.5. This is not the case for the most upper regions above $3h$ and the lowest region near the midplane. For the most upper region, it is known that the settling velocity is fast compared to the lower regions. Particle 4h in figure 4.1b falls down from 4h to 3h in about 25 years and reaches the 'middle region'. Within a few years, all particles have departed from the upper region, and there are no more particles

(a) Dust density at $r = 1$AU

(b) Dust density at $r = 10$AU

(c) Dust density at $r = 50$AU
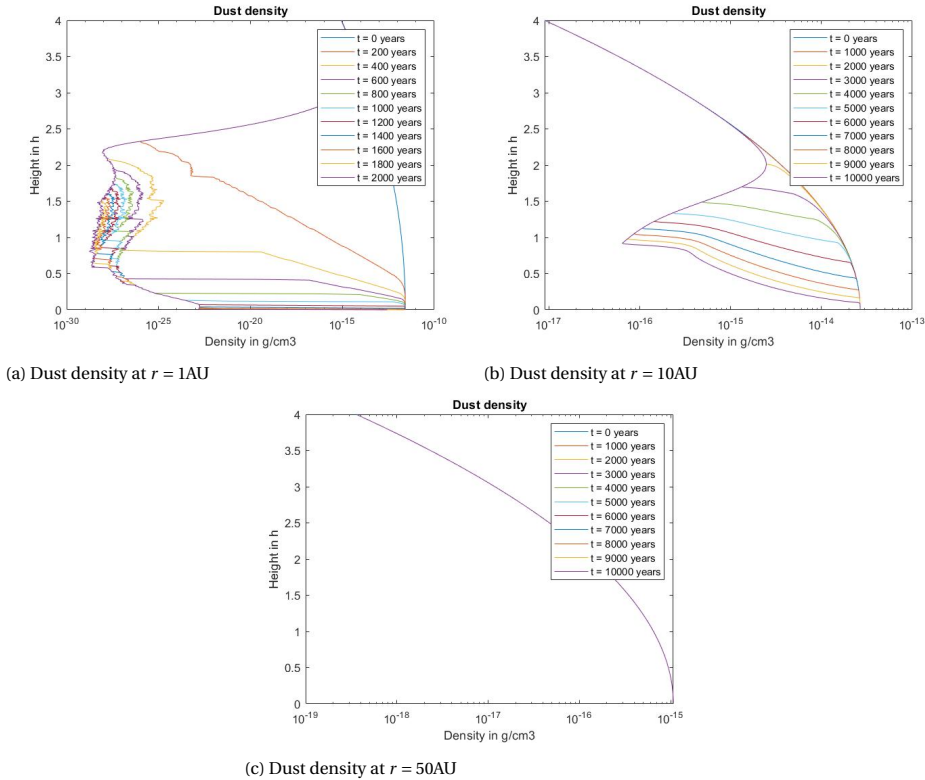
Figure 4.3: The upper left figure represents the dust evolution for $r = 1$AU, the upper figure on the right represents the dust evolution for $r = 10$AU and the lower one for $r = 50$AU.

left to consume the dust. So, the fact that the dust does not decrease much in the upper regions is due to the fact there is nothing left to 'grow from the dust' and the dust remains constant.

For the dust density at $r = 50$AU, the dust does not change for the whole vertical profile. This is the result of the little growth of the particles. In farther regions, the dust density is already thinner and therefore, there is less material for the particles grow. The settling velocity is not directly impacted by the radial distance from the star, but the particles settle less due to the fact that they are small and do not grow. So, due to the little growth of particles, the dust remains constant in these regions.

PARTICLE DENSITY
Particle densities for each radii are given in figure 4.4.

The left hand column represents the density of particles over time. Figure 4.4a shows the densities at $r = 1$AU. More specifically, it is possible to observe when a particle collides, or gets eaten by a larger particle, as this evident from sudden decreases in density. For instance, the line for particle originating from 1h in figure 4.4a, experiences a sudden decrease in density at about 200 years. This is due to an encounter with a larger particle.
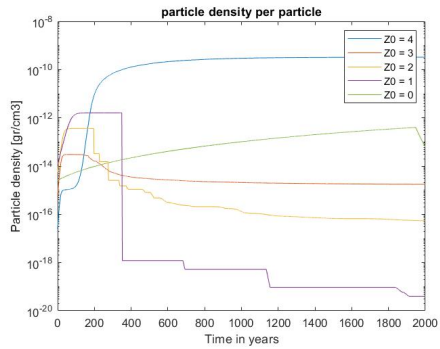
(a) Particle density versus time at $r = 1$AU
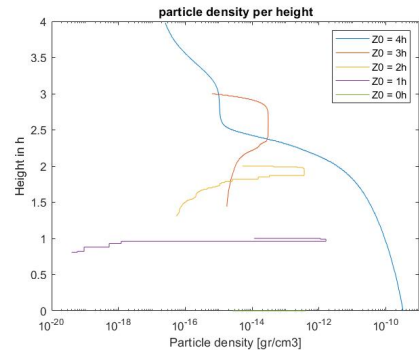
(b) Particle density versus height of the particle at $r = 1$AU
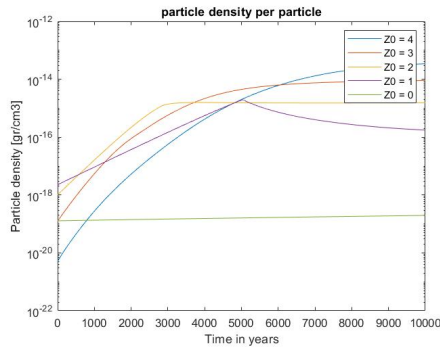
(c) Particle density versus time at $r = 10$AU
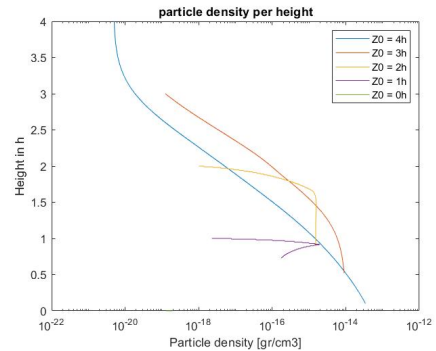
(d) Particle density versus height of the particle at $r = 10$AU
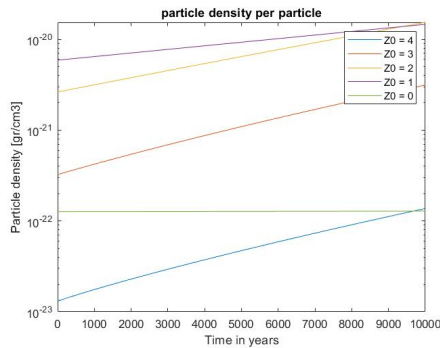
(e) Particle density versus time at $r = 50$AU
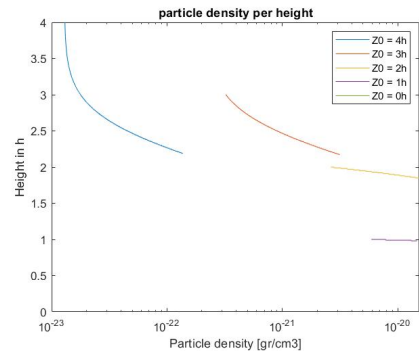
(f) Particle density versus height of the particle at $r = 50$AU

Figure 4.4: The upper left column of figures represent the density of the particles over time for each particle, indicated by different coloured lines. The right hand column of figures represents the particle densities over height for each particle. As the particle settles, their densities either increase by growing, or decrease by being fed to larger particles.

The larger particle 4h can be seen growing where there are no drops in the density. This means that it is only encountering particles which is smaller than itself, and will only grow as a result from the encounters.

The right hand column of figure 4.4 represent the density of particle families over height. With these figures, location of encounters between particles can be observed. For instance in figure 4.4b, an encounter between the particle families from 4h and 2h is visible at a height of about 2h. Particle 4h is larger and will feed on the particle 2h. This results in a steep decrease in density for particle 2h and growth for particle $4h$.

For the radius at 50AU, the initial densities are very low compared to 1AU or 10AU. Knowing that there is very little growth and settling, there are few encounters between particles. This can be seen in the lines where there is little change in the left column of figures. The right hand column shows how the particles do not reach the height of other particle, and no encounters are present.

4.2.2. RESULTS WITH GAS DECAY

Within a PPD, gas decay is a process that is observed via observations. The decay of gas results in the disk's disappearance and is a process that is estimated to require shorter time-scale relative to the entire planet formation. According to Mamajek [17], observations show that PPDs do not last longer than several millions of years. After this time-scale, disks are not observed any more, or are only a small fraction of their initial size. This gas decay is the result of different processes. One of them is the called photo-evaporation and is the process where gas is ionised by energetic radiation from the central star. The gas will disperse away from its initial position. The molecules and atoms in the gas rise in temperature and are therefore accelerated. If the photon has sufficient energy, it is possible for the gas to reach velocities beyond the local escape velocity. The gas will get ejected from the system and the PPD will be thinner.

Using a collection of star systems, it was observed that the gas decay of PPDs follows an exponential function. In this thesis, the following formula is used to model that gas surface density as a function of time and radial distance from the central star [18]:

$$\Sigma_{gas}(r, t) = \beta_0 e^{-t/\tau_{disk}} \left(\frac{r}{AU} \right)^{-1} \tag{4.1}$$

Where β_0 is the surface density at 1 AU, τ_{disk} is the disk lifetime, t is the time, r is the radial distance from the central star. To visualise the effect of the gas decay figure 4.5 is given. It visualises the gas density over a period of 2500 years, at 1AU, using a $\tau_{disk} = 500$ years.

PARTICLE GROWTH

Enforcing equation 4.1, to change the gas density over time in the program yields change in the settling process as it is dependent on the gas density. As time passes, the gas density decreases, which allows for the particles to experience less drag when settling. The new results are given in figure 4.6.

Figure 4.6 shows the evolution of the particles where gas decay is incorporated. Furthermore, the program is run for a period of 1000 years for the scenario at $r = 1$AU and 3500 years for the scenarios at 10AU and 50AU. The reason for the different timescale is to use a timescale in which the particles are able to arrive at the midplane.

From figure 4.6 it can be seen that the growth of the particles has changed compared to the scenario without gas decay.
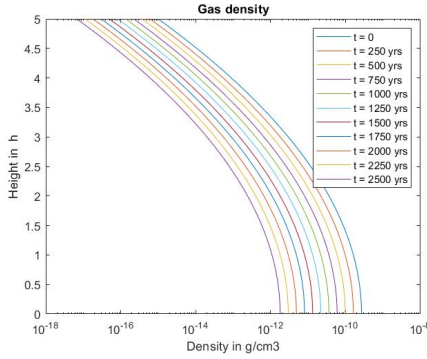
Figure 4.5: The vertical gas profile at a radius of 1AU. The gas profile decays as time moves due to the gas decay model enforced in equation 4.1. Here τ_{disk} is 500 years.

At r = 1AU, the changes are not as prominent. The largest particles grow into similar sizes as the ones without gas decay, growing into about 250 microns. However, the changes are seen in the settling which is faster. Particles settle faster as a result of the decreasing drag, as gas is dissipating. Without gas decay, the largest particle would require about 1600 years to arrive at the midplane, while in this scenario, only 700 years are required.

The figure for r = 10AU shows the effect of gas decay more clearly as the settling again is faster than the standard scenario. The largest particles require about 1500 years to settle onto the midplane, and majority of the particles have settled onto the midplane after about 3000 years. It can also be observed that the growth does not initiate after about $500 - 1000$ years, where the line remains slightly flat. This shows the effect of gas drag which does not allow for much growth in the early years. As the gas dissipates, particles are able to settle more efficiently, collide, and grow, which is then seen as the steep increase in growth after 1000 years for the largest particle.

At r = 50AU, particles grow into larger sizes compared to the situation without gas decay. The largest particle reach sizes of about 45 microns. As can be seen, the change in gas density allows for sudden increases in growth for the particles as there is less gas drag obstructing their vertical movement. Also here, the particles take some time before they can settle, about 2000 years. Here the initial gas density was too much for the particles to settle. Once the gas decayed, they were able to settle.

DUST EVOLUTION
Figure 4.7 visualises the evolution of the dust density for each radial distance and with gas decay incorporated. For r = 1AU and r = 10AU, the figures are similar to the ones from figure 4.3 where the middle region decreases drastically while the top and bottom region remain constant. The middle region is where most particles grow and thus most dust is used for the growth of the particles.

The dust density at r = 10AU has similar features with some differences. The upper half above 2.5h is constant while the lower half has decreased. Then, the bottom region near the midplane is depleted in this case. In figure 4.6c and d, it can be seen that the
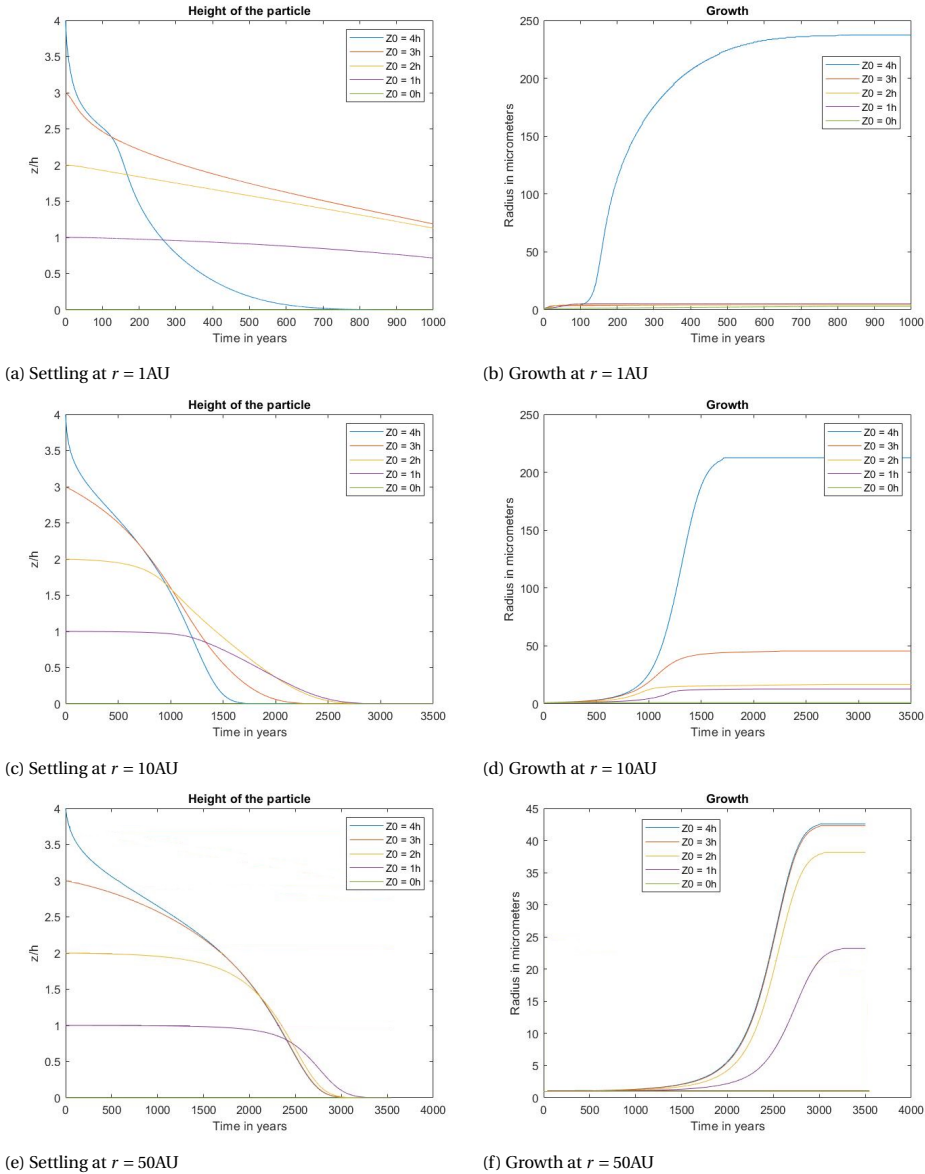
Figure 4.6: Each row represents results from a different radial distance from central star. The upper row stands for 1AU, second row for 10AU, the third row for 50AU. left) the settling of particles towards the midplane. Each line represents a particle starting from a height. Right) The growth of the particles when settling onto the midplane. Each line represents one particle starting from a height above the midplane.

growth of particles initiates after about 1000 years. The largest particle has already arrived at about $z = 1.5h$ after 1000 years. Most particles are already at the lower regions when growth excels, this means that the dust in the lower regions will be depleted due to

(a) Dust density at $r = 1$AU

(b) Dust density at $r = 10$AU

(c) Dust density at $r = 50$AU
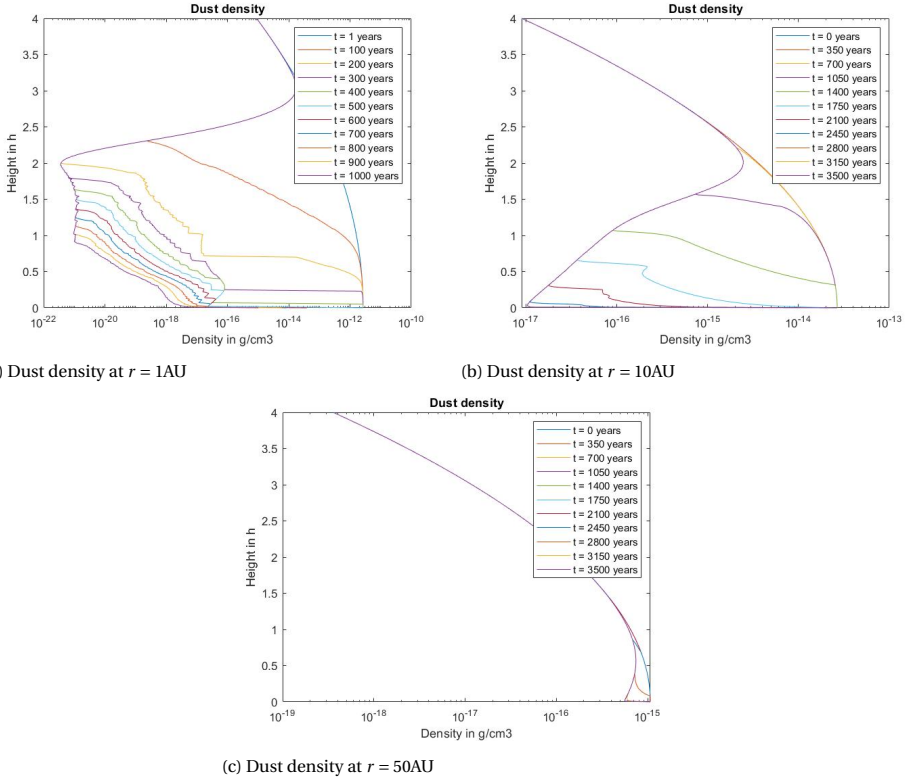
Figure 4.7: The upper left figure represents the dust evolution over $r = 1$AU, the upper figure on the right represents the dust evolution at $r = 10$AU and the lower one for $r = 50$AU.

growth of the particles as most particles are located in that region.

The dust density at $r = 50$AU, shows some decrease in dust at the lower regions. This is due to the fact that growth of the particles takes place after 2000 years. In figure 4.6e and f, the growth of the particle would only initiate after about 2000 years. Figure 4.6e then visualises that the largest particles is already located at about $z = 2h$. After 2500 years, most particles are located under $z = 1h$. So, during the growth of particles, most particles are located near the midplane. This means that the regions near the midplane gets depleted, and the upper region remains constant as there are no particles to grow over there. Furthermore, the decrease in dust is little compared to the decrease in $r = 10$AU or $r = 1$AU. This is due to the fact that the most dominant factor for the growth of particle is the smaller particles. The dust does not play a large role in this part as seen in the density.

PARTICLE DENSITY
Figure 4.8 is similar to figure 4.4 where the particle densities are visualised. The figures for $r = 1$AU and $r = 10$AU, figure 4.8a, b, c and d are very similar. The growth of the density of particles can be seen, the largest particle is able to grow from smaller particles,
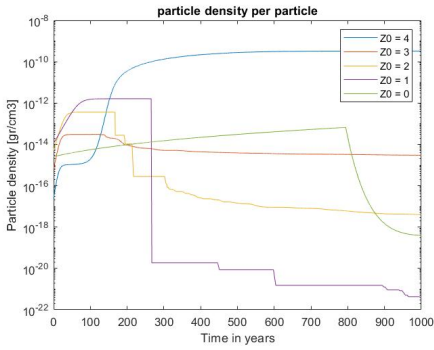
(a) Particle density versus time at $r = 1$AU
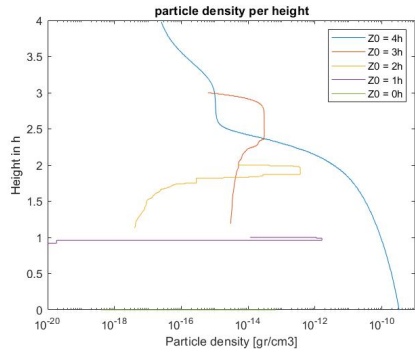
(b) Particle density versus height of the particle at $r = 1$AU
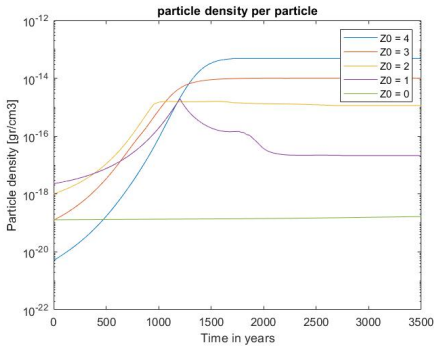
(c) Particle density versus time at $r = 10$AU
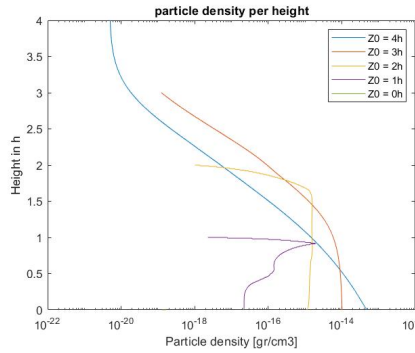
(d) Particle density versus height of the particle at $r = 10$AU
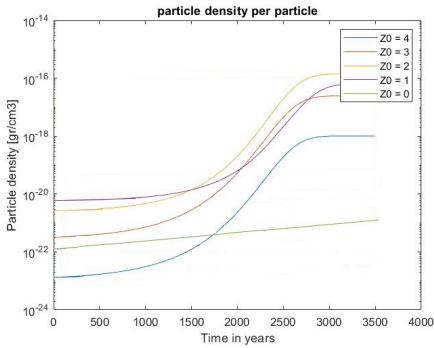
(e) Particle density versus time at $r = 50$AU
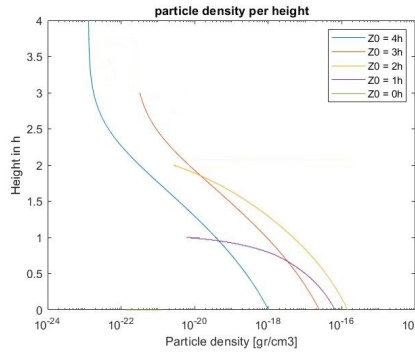
(f) Particle density versus height of the particle at $r = 50$AU

Figure 4.8: The upper left figure represents the particle density evolution over $r = 1$AU, the upper figure on the right represents the particle density evolution at $r = 10$AU and the lower one for $r = 50$AU.

and smaller particles are fed to larger particles which is evident from the drops in density.

Figure 4.8e and f visualise the particle density for $r = 50$AU. Where growth can be seen, and decreases are not seen. This means that all particles visualised are growing and do not encounter each other, while other particles which are not visualised are fed

into these particles.

4.2.3. RESULTS WITH TURBULENCE

A third model which is considered, a turbulence model. In this model, there is no gas decay and an additional turbulent velocity is enforced. With this additional velocity, the particles are able to grow as the particles are able to sweep the dust and other particles with the higher turbulent velocity. A simple turbulence model is implemented in this program alongside the settling behaviour and this also means that the growth of the particles will not be dominated by the settling anymore as largest source of relative velocity is now the turbulence. According to Nomura et. al [19], there exist global turbulent motions in the disk, which is in the order of $v_{turbulent} \approx 0.1 c_s$ for strongly turbulent disks.

The growth for each particle is then calculated as:

$$\frac{dm}{dt} = \pi a^2 v_{turbulence}(\rho_d + \rho_p) \tag{4.2}$$

PARTICLE GROWTH

For the figures in first row in figure 4.9, the growth of particles is given the particle families originating from $4h, 3h, 2h, 1h$ and specifically $2.64h$. This particle family $2.64h$ is visualised in the figure as it has grown most and has eaten most other particles. The final radius of the particle is about 1.7 millimetres. The following details can be found from the growth:

- The growth of the particles is little dependent on the dust density and and most dependent on encounters with other particle families. This can be seen from the fact that particles from higher up, for instance from $4h$ do not result in the largest particles. From the previous subsections, it was established that most encounters occur in the middle region as that is the region where most particles are located. This is the result of particles settling, but encountering the gas density as a barrier to overcome before settling further downwards. As particles are blocked by the gas drag from settling, more and more particles will be concentrated in this region and encounters among particles occur where one grows from the other. Large growth is then possible in this region. However, the particles from higher up, need time before they arrive in this region, and by the time they arrive in this region, other particles have already grown into larger sizes. This results in the particles from higher up being eaten by the larger grown particles and is the reason why particles from higher regions do not grow in this scenario;

- One particle family from one height, has eaten the majority of all other particles and dust. This is the result of the large growth for the particle family as the large turbulent velocities allows for more mass gain. However, this also means that there are large mass losses for other particle families which are eaten by larger particles families. When this happens, smaller particle families are (nearly) fully eaten by larger particles families and little of the smaller particle families are left. This results in a situation where, at the end of the simulation, there is only one large particle family, and the smaller families which were not fully eaten;

(a) Settling at $r = 1AU$

(b) Growth at $r = 1AU$

(c) Settling at $r = 10AU$

(d) Growth at $r = 10AU$

(e) Settling at $r = 50AU$

(f) Growth at $r = 50AU$
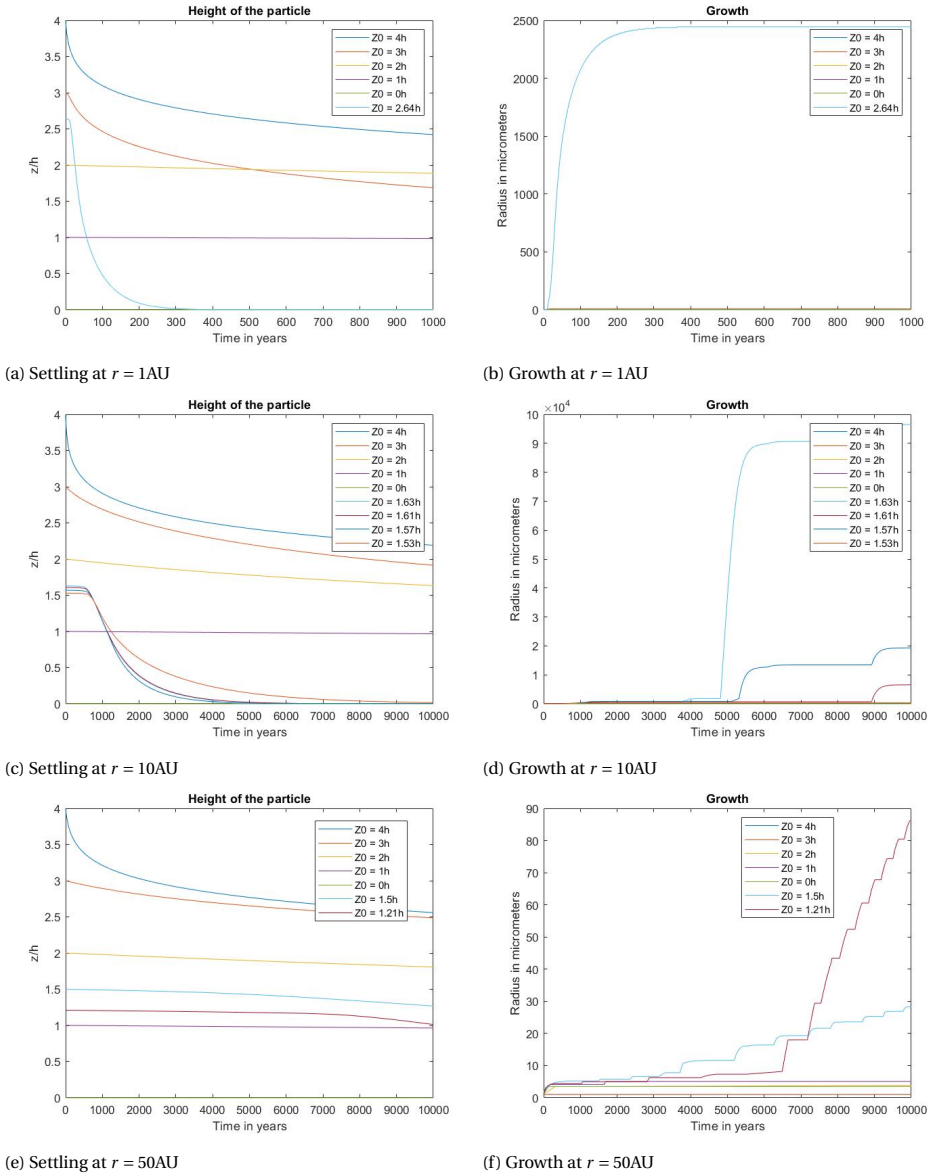
Figure 4.9: Each row represents results from a different radial distance from central star. The upper row stands for 1AU, second row for 10AU, the third row for 50AU. left) the settling of particles towards the midplane. Each line represents a particle starting from a height. Right) The growth of the particles when settling onto the midplane. Each line represents one particle starting from a height above the midplane.

- At 10AU, this phenomenon where only one particle family would grow and others are eaten, occurs as well, but at a later timescale and several particles large particle families from different heights emerge instead of only one family. This is the

result of fewer encounters between particles as growth itself is not as prominent in farther regions because of the smaller dust and gas density. When there are less encounters among particles, a single particle family is not able to encounter and eat all other particles. Eventually, the largest particles families arrive at the midplane and will feed on each other. This results in large and rapid growth for the largest particle families as the largest particles encounter each other. The difference between this scenario and the one from $r = 1$AU, is that the largest particle families encounter each other, instead of the largest particle family encountering all other (small) particles. Largest growth can occur from encounters between large particle families, and as a result, a particle with a size of about 9 centimetres emerges at $r = 10$AU;

- At 50AU, the particles are not able to grow and settle due to the lack in dust and gas. The largest particles grew into a size of nearly 90 microns. As particles are not able to grow and settle, no encounters occur and this results in little growth as well. This can be seen in the figure where the settling of the particles barely occur, and there is also little growth.

DUST EVOLUTION

The dust evolution is given in figure 4.10. The dust density will be eaten instantly due to the high growth rate of the particles. As every particle is under the influence of high relative turbulent velocities, the decrease in dust density is large. Large enough for the dust to disappear in a few years. This is seen in the figure where the lines for later timesteps move to zero, This is applicable for each radial distance, in this case the r at $1, 10, 50$AU are visualised.

PARTICLE DENSITIES

Figure 4.11 visualises the densities of particle families starting from different altitudes above the midplane. The left hand column represent the densities over time, and the right hand column represents the densities over height.

- At 1AU, the largest particle is visualised in figure 4.11a and b. The figures visualise the particle family $2.64h$ feeding from every other particle. In figure 4.11a, particle family $2.64h$ is able to grow continuously without losing mass. In figure 4.11b, particle family $2.64h$ is able to feed from other particle families. When crossing heights with particle family $2h$, the density of of particle family $2.64h$ is able to feed from particle family $2h$. This causes the density of particle family $2h$ to decrease which is seen as the horizontal line. Particle family $2.64h$ is able to grow and settle continuously where it will encounter other particles;

- At 10AU, it can be seen that the largest particle families reach the midplane in figure 4.11d and a after about 5000 years. This is the region where the largest particle families feed from each other, and only one family is able to come on top, which is family $1.63h$. This can be seen in figure 4.11a where several large particle families ($1.57h$ or $1.61h$) drop in density between times 4000 and 5000 years. As they arrive onto the midplane, they are eaten by the largest particle 1.63h.

(a) Dust density at $r = 1$AU

(b) Dust density at $r = 10$AU

(c) Dust density at $r = 50$AU
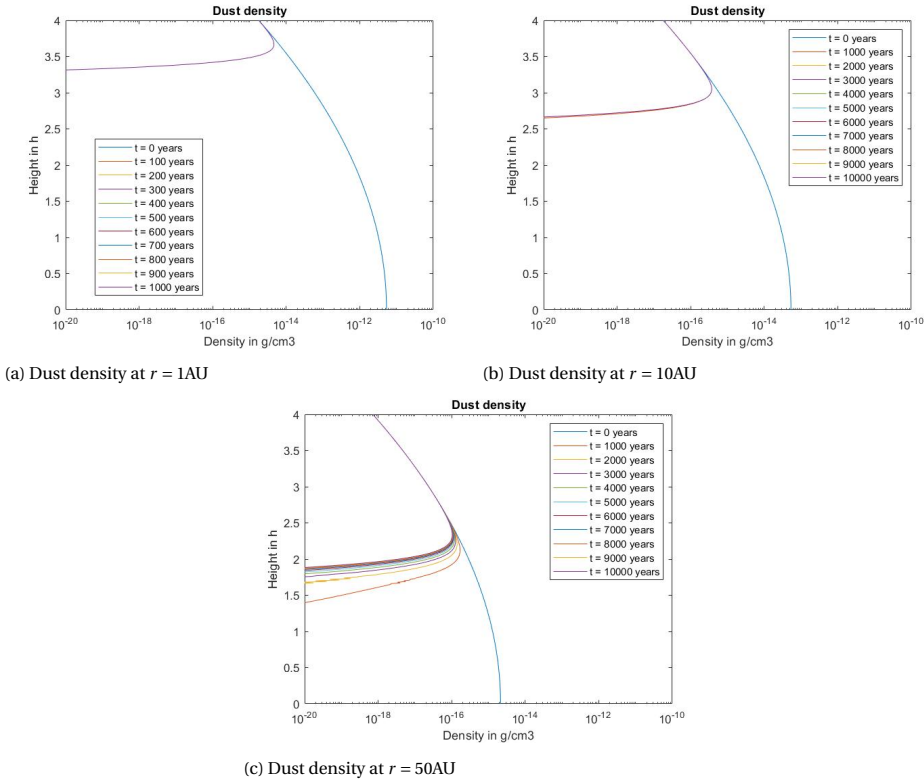
Figure 4.10: The upper left figure represents the dust evolution over $r = 1$AU, the upper figure on the right represents the dust evolution at $r = 10$AU and the lower one for $r = 50$AU.

- At 50AU, there is little growth and encounters as seen in the figure 4.11f and g. Encounters do occur but at not as frequent. In figure 4.11a, it can be seen that particle families $4h$ and $3h$ remain constant over the 10000 years, meaning that they had no encounters as the density remained constant. Particle families $1.5h$ and $1.21h$ are visualised in figure 4.11f and g as well, as these two are the only growing particle families. In figure 4.11g, their vertical movement is shown, and it can be seen that these particles were only present in the lower regions of the disk. This means that these particle families only fed from the lower region particles, and do not reach large sizes, even though these are the largest particle families.

4.3. CONCLUSION ON PEBBLE FORMATION

In this section, the particles are evaluated based on the two definitions defined in this chapter. Based on the definitions, it is determined whether or not pebbles pebbles are formed after settling and coagulation.
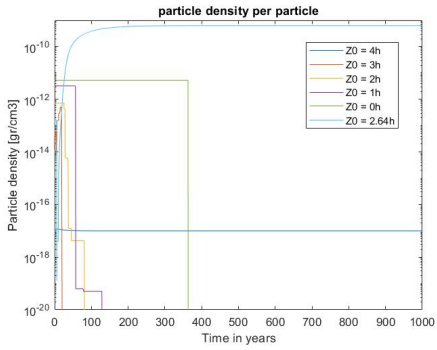
(a) Particle density versus time at $r = 1$AU
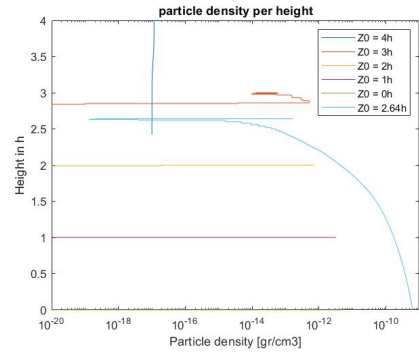
(b) Particle density versus height of the particle at $r = 1$AU
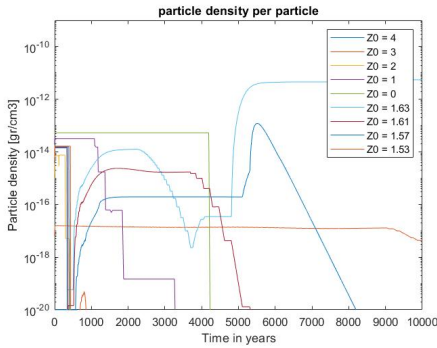
(c) Particle density versus time at $r = 10$AU
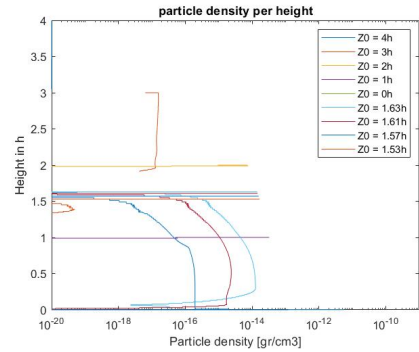
(d) Particle density versus height of the particle at $r = 10$AU
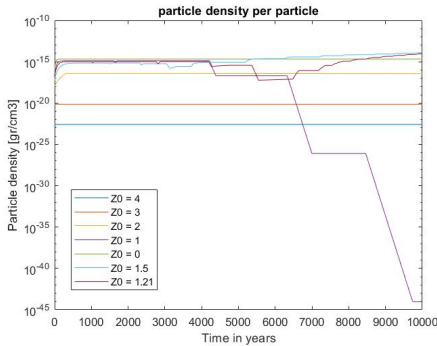
(e) Particle density versus time at $r = 50$AU
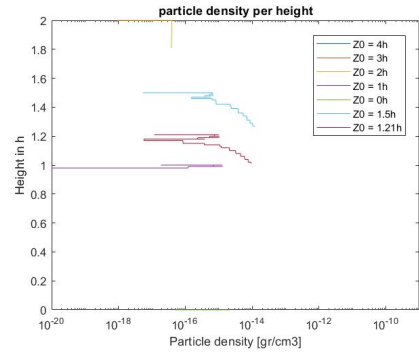
(f) Particle density versus height of the particle at $r = 50$AU

Figure 4.11: The upper left figure represents the particle density evolution over $r = 1$AU, the upper figure on the right represents the particle density evolution at $r = 10$AU and the lower one for $r = 50$AU.

BASED ON M. LAMBRECHTS DEFINITION OF PEBBLES

Lambrecht's definition for a pebble states that a particle needs to have a radius of at least 1 mm and based on this criterion, pebbles are not formed as no particles reached the 1 mm threshold. The largest particles formed without gas decay were located at 1AU

with a radius of about 120 microns. With gas decay, the largest particles were found at 10AU with a radius of about 225 microns. Next, with the turbulent case, some particles were able to eat all other material and resulted in large particles, larger than *cm*.

BASED ON C. ORMEL DEFINITION OF PEBBLES

Chris Ormels definition [3] includes limits for the Stokes numbers. The Stokes numbers of the particles are plotted in figure 4.12.
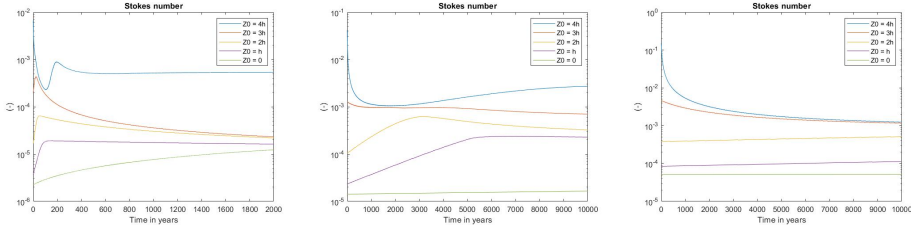
(a) Stokes numbers at $r = 1AU$ without gas decay
(b) Stokes numbers at $r = 10AU$ without gas decay
(c) Stokes numbers at $r = 50AU$ without gas decay
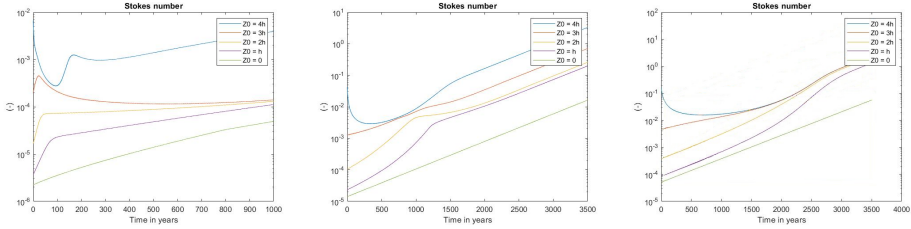
(d) Stokes numbers at $r = 1AU$ with gas decay
(e) Stokes numbers at $r = 10AU$ with gas decay
(f) Stokes numbers at $r = 50AU$ with gas decay
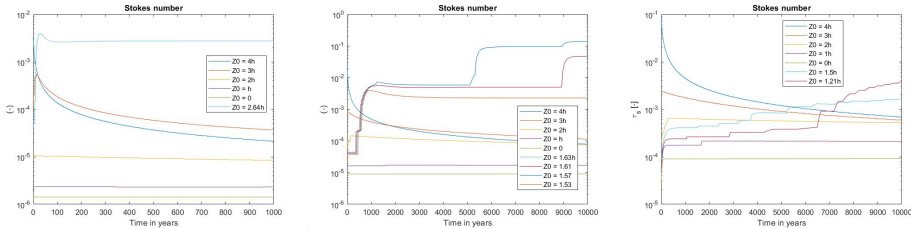
(g) Stokes numbers at $r = 1AU$ for the turbulent case.
(h) Stokes numbers at $r = 10AU$ for the turbulent case.
(i) Stokes numbers at $r = 50AU$ for the turbulent case.

Figure 4.12: The Stokes numbers of the particles. The first row represents the particles from the standard scenario, the second row represents the situation with gas decay, and the last row represents the turbulent case. Each for a different timescale.

Figure 4.12 visualises the stokes numbers for three different distances from the central star. The upper row represents the simulation without gas decay and the lower row for the simulations including gas decay. It can be seen that the stokes numbers are increasing for the gas decay scenario. As the gas density decreases, the particles experience less drag which allows them to be decoupled to the gas. This is reflected in an increase in Stokes number. However, this means that the upper limit of Ormels criterion will even-

tually be reached, no more pebbles are present.

As Ormel described, particles are considered pebbles when they have stokes numbers between 10^{-3} and 1. For each scenario, the following conclusion can be made:

For *r=1* AU without gas decay, there are no pebbles. As most particles have a stokes number smaller than 10^{-3}. The gas is too thick and the particles are too coupled to the gas;

For *r=10* AU without gas decay, pebbles are formed as the particles from $4h$ and $3h$ have stokes numbers larger than 10^{-3} and lower than 1. The gas in this region is thin enough and pebbles are formed;

For *r=50* AU without gas decay, pebbles are also formed. The particles from $4h$ and $3h$ have stokes numbers larger than 10^{-3} and lower than 1. Just as at $r = 10$AU, the gas is thin enough and pebbles are formed and just as at $r = 10$AU;

For all cases with gas decay, pebbles are only formed temporarily. This is due to the increase in Stokes number as gas decays. For longer timescales, Stokes numbers will have reached the upper limit of Ormels criterion and no more pebbles will be present. So, no pebbles are formed as the Stokes numbers will increase beyond the upper limit;

For *r=1* AU with turbulence, the particle family which was able to eat all other particles has Stokes numbers of about 0.7 [−]. So from the Stokes number, pebbles are formed;

For *r=10* AU with turbulence, the largest particles are also able to reach Stokes numbers between 10^{-2} and 10^0, pebbles are formed;

For *r=10* AU with turbulence, the particles are also able to reach Stokes numbers between 10^{-2} and 10^0, pebbles are formed as well.

4.4. DO WE FORM PEBBLE?

Based on the previous sections, it can be seen that pebbles are formed based on the criterion and distances from the central star. For the Lambrechts criterion where particles need to reach $1\ mm$, pebbles are formed in the turbulent model. For the other models, no pebbles were formed due to a lack of growth. No particles were created in the simulations gas decay and standard model as the growth of the particles was not enough for them to reach the $1\ mm$ size. The lack of growth can be influenced by the following parameters:

- Larger initial sizes allow for more growth and more settling;

- Less gas drag could be a solution which was explored by applying the gas decay model. It allowed for larger growth of the particles as there is less drag when settling downwards. This resulted in larger particles;

- For the turbulent case, some particle families were able to reach centimetre sizes. Some pebbles are formed.

For C. Ormels criterion, pebbles were formed:

- Without gas decay, pebbles are formed in farther regions from the central star. As gas density decreases over radial distance, the lower gas density in farther regions allows for the Stokes numbers of the particles to meet the criterion. For each radius, most particles which meet this criterion originate from initial higher altitudes. So, most of the particles are the larger particles which were able to settle and grow;

- With gas decay, pebbles are also formed temporarily. This is due to the gas decay over time, which increases the Stokes numbers over time. The simulation in figure 4.12c - d shows the Stokes numbers up to a time of 3500 years. However, at later years Stokes numbers will have reached orders of 10^4 due to the low gas density. In this case, no pebbles are formed;

- In the turbulent case, growth during settling was more efficient and larger particles were formed. This was reflected in the Stokes numbers as most of the larger particles had Stokes numbers between 10^{-3} and 1 [-]. Pebbles were formed throughout the disk.

EFFECT OF OTHER PARAMETERS

One solution which can be enforced is to use a smaller gas decay. In this scenario, the gas decay model was following equation 4.1 with τ_{disk} of 500 years, which is unrealistic. This results in the decrease in gas density and also the increase in stokes number. If the gas density were to decrease less rapidly, the stokes numbers would not reach the upper limit as fast and would remain pebbles. However, changing the gas decay can be delicate as the rapid decrease of gas allowed the particles to grow in the first place. A suitable balance in gas decay needs to be found where the particles are allowed to grow, yet do not reach the upper stokes number criterion.

5

RADIAL MOVEMENT

The previous two chapters described the process of particles settling onto the midplane. Once the particles arrived on the midplane, settling of particles ceases to exist and other forces come into play. This is the process which results into radial movement of the particles towards the star and is described in this chapter. In section 5.2, the physics involved in the radial movements of particles is explained, and in section 5.3 the results of particles flux in the disk and how the mass of particles are distributed within the disk is shown.

5.1. THE INITIAL DISTRIBUTION OF MASSES

From the models performed in the last chapter, the density of dust and particles in the disk can be obtained. This is shown in figure 5.1:
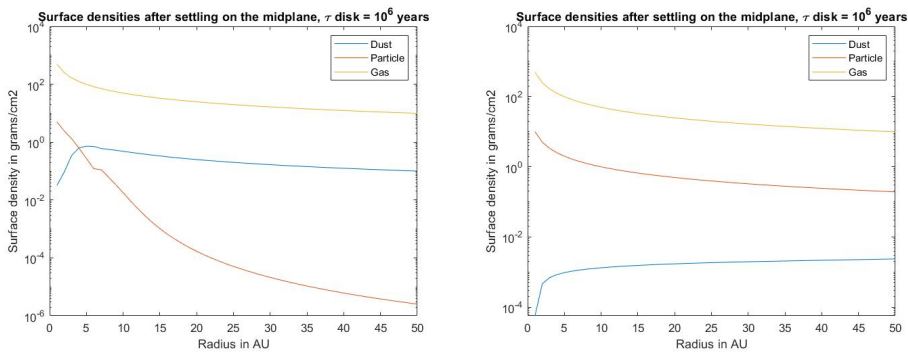
Figure 5.1: The surface density of dust, gas and particles after settling onto the midplane

Figure 5.1 encapsulates the current results over the radial distance for both the standard settling and coagulation scenario, and the turbulent scenario. The gas decay model is not taken into consideration because of the large Stokes numbers. These results are

the initial conditions in the disk before radial movements are taken into account, which will alter these distribution.

5.2. RADIAL DRIFT OF PARTICLES

Small particles with radii of under a centimetre, are tightly coupled to the surrounding gas. Unlike the gas, these small particles do not experience the radial pressure gradient and will experience a net inwards force. This effect allows the particles to radially drift.

The difference between the gas and Keplerian velocities is calculated. This is the velocity at which the gas is rotating, which is sub-Keplerian. The force balance is given as [4]:

$$\frac{v_{\Phi,gas}^2}{r} = \frac{GM_\star}{r^2} + \frac{1}{\rho}\frac{dP}{dr} \tag{5.1}$$

Where the term on the left hand side is the rotational gas velocity, the first right hand term is the Keplerian component and other term is the azimuthal pressure gradient. The pressure on the midplane is approximated as a radius power-law:

$$P = P_0 \left(\frac{r}{r_0}\right)^{-n} \tag{5.2}$$

Where $P_0 = \rho_0 c_s^2$. n is the power-law index and is positive as pressure decreases outwards. The rotational gas velocity can now be calculated as:

$$v_{\Phi,gas} = \sqrt{\frac{GM_\star}{r} - c_s^2 n} \tag{5.3}$$

Where c_s is the thermal velocity. Using the substitution η which is a measure of the gas pressure support [20]:

$$\eta = n\frac{c_s^2}{v_k^2} \tag{5.4}$$

Yields the rotational gas velocity as:

$$v_{\Phi,gas} = v_k \left(1 - \eta\right)^{\frac{1}{2}} \tag{5.5}$$

Equation 5.5 describes the rotational velocity of the gas, which is slightly lower than the local Keplerian velocity. As an example, the rotational velocity for a disk with $h(r) = 0.05r$, surface density profile $\Sigma \propto r^{-1}$ where $n = 3$ [4], the rotational velocity is calculated as:

$$v_{\Phi,gas} \approx 0.996 v_k \tag{5.6}$$

Based on equation 5.6, the rotational gas velocity is slower by 0.3% from the Keplerian velocity. This velocity, as function of radius, is shown in figure 5.2 and compared with Keplerian velocity.

The difference is small at first look. However, at $r = 1$AU, the difference is calculate to be around $120\frac{m}{s}$. Meter sized rocks moving at $1AU$ experience the gas then as drag.
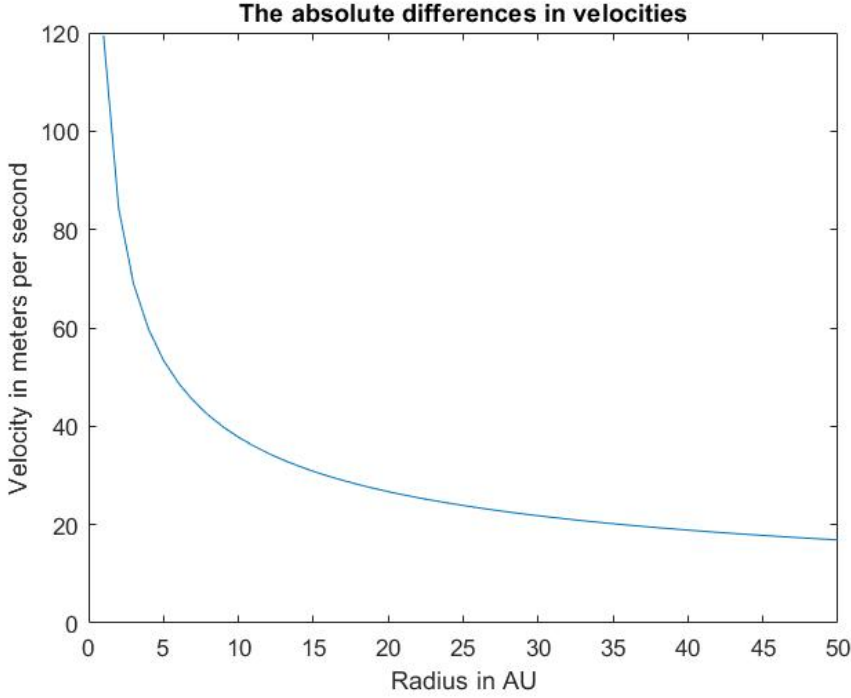
Figure 5.2: The absolute differences in the rotational gas velocity and the Keplerian velocity.

The azimuthal velocities of particles are different from the velocities of the gas. The difference is experienced by the particles as drag from the gas, which moves the particles in the radial direction. If there were no gas, the particles would orbit with the Keplerian velocity. The radial and azimuthal equation are given as [4]:

$$\frac{dv_r}{dt} = \frac{v_\Phi^2}{r} - \Omega^2 r - \frac{1}{t_{fric}}(v_r - v_{r,gas}) \tag{5.7a}$$

$$\frac{d}{dt}(r v_\Phi) = -\frac{r}{t_{fric}}(v_\phi - v_{\phi,gas}) \tag{5.7b}$$

Where v_r and v_Φ are the radial and azimuthal components of the velocity. The terms in equation 5.7a are in order: the centripetal acceleration, the gravitational acceleration and the gas drag. The t_{fric} is the friction timescale. Assuming that the gas and particles are close to the Keplerian velocity: $v_{\Phi,gas} \approx v_\Phi \approx v_k$, which means that the particles spiral inwards through successions of nearly circular, nearly Keplerian orbits, then [21]:

$$\frac{d}{dt}(r v_\Phi) \approx v_r \frac{dt}{dr}\frac{d}{dt}(r v_\Phi) \approx v_r \frac{d}{dr}(r v_k) \approx \frac{1}{2} v_r v_k \tag{5.8}$$

Substituting equation 5.8 into equation 5.7b:

$$v_\Phi - v_{\Phi,gas} = -\frac{1}{2}\frac{t_{fric}v_r v_k}{r} \tag{5.9}$$

For the radial equation 5.7a, equation 5.5 is used for Ω. Neglecting the higher order terms of order $(h/r)^4$ and higher, equation 5.7a is reduced to:

$$\frac{dv_r}{dt} = -\eta\frac{v_k^2}{r} + \frac{2v_k}{r}(v_\Phi - v_{\Phi,gas}) - \frac{1}{t_{fric}}(v_r - v_{r,gas}) \tag{5.10}$$

The left hand side is of the order v_r^2/r and is assumed to be zero if $v_r << c_s$ which is the case here. Also, it is assumed that $v_{r,gas} << v_r$ which is true for most particles in orbital decay. From equation 5.9 and 5.10 the radial velocity of the decaying particle over the Keplerian velocity can be calculated as:

$$\frac{v_r}{v_k} = -\frac{\eta}{\frac{v_k}{r}t_{fric} + \frac{r}{v_k t_{fric}}} \tag{5.11}$$

Isolating the radial velocity and introducing the Stokes number τ_s, equation 5.11 is reduced to:

$$v_r = -\frac{\eta v_k}{\tau_s + \tau_s^{-1}} \tag{5.12}$$

Equations 5.11 and 5.12 are visualised in figure 5.3.
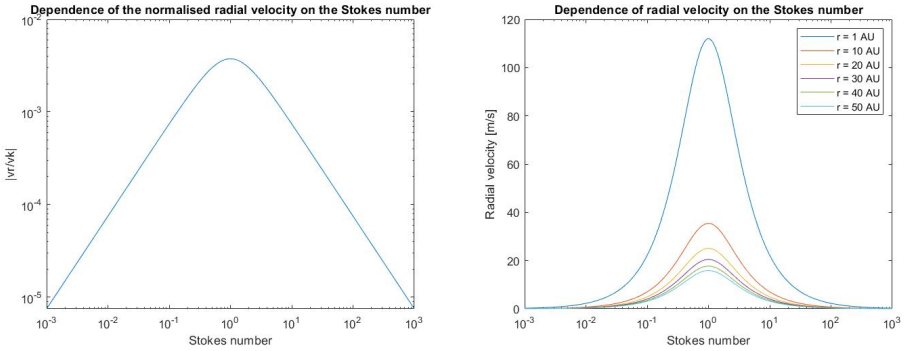
Figure 5.3: Left) the normalised radial velocity of particles. The line represents the radial velocity over the local Keplerian velocity. The shape of the line implies that the largest radial is obtained at Stokes number of 1. Right) the radial velocity at each radial distance. Each line represents the velocity of particles with Stokes numbers at a particular radius.

Figure 5.3a visualises the dependence of the radial velocity of particles on their Stokes numbers. Particles attain their largest radial velocity when $\tau_s = 1$. This means that the friction timescale equals the orbital period; the velocity is then independent of the disk properties. As described in chapter 3, the Stokes number is a function of the radius, gas density, material density and the thermal velocity. The radius is important as it is the

only variable physical property of the particle (other than its material density). Translating the dependence of the Stokes number on the physical radius of the particle, it is understood that larger particles have larger radial velocities than smaller. Generally, the peak radial velocity at a distance of a few AU is obtained by particles with radii of a few *cm* to a few *m*. This means that particles which are much smaller than those sizes, have much smaller radial velocity and radial drift is severely slow. This is due to the fact that small particles are coupled to the gas, the gas severely suppresses their radial movement. At the midplane where the gas is most dense, this effect is most prominent.

Figure 5.3b plots the radial velocity of particles dependent on the Stokes number and the radius from the central star. The velocity is largest closest to the star and decreases outwards. It is now possible to associate particles with certain Stokes numbers with their radial movements.

5.3. RESULTS

The following section discusses the results obtained from the radial movement of particles.

RADIAL MOVEMENT

The particles which were settling in the previous chapters, have arrived onto the midplane and are subjected to radial movements explained in the previous section. Figure 5.4 represents the radial movement of the largest particles at each radial distance as these ones are the ones with the largest radial movement:
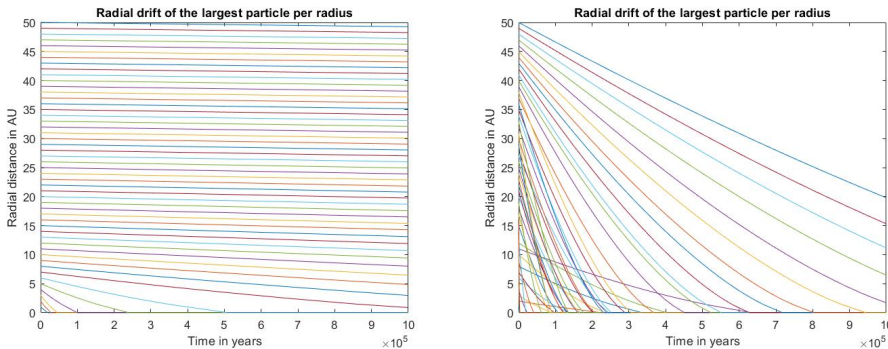
(a) The radial drift of the largest particle for the standard settling and coagulation scenario.

(b) The radial drift of the largest particle for the turbulent scenario.

Figure 5.4: The radial movement of the largest particle at each radius. The vertical axis represents the distance from the central star and the x axis represents the time in years. The left panel is represents the standard settling and coagulation panel and the right panel represents the turbulent growth scenario. Each line in the figure represents the position of the particle due to drifting.

Figure 5.4 visualises the radial movement of the largest particle at each radius. This means that the particle which grew largest at each radius was used for the calculation of the radial drift. The largest particle results in the largest radial movement as mentioned in the previous section.

Movement for the standard scenario

In this figure 5.4a, the standard scenrio, radial movement is observed from the particles which start at radial distances near the central star. However, it can also be seen that most particles barely move radially and most of them stay in place or move very little. Especially for particles which start at higher radial distances where the lines are horizontal for the entire time, meaning that radial movement is nearly non-existent.

For example, the particle starting from $r = 40 AU$, with radius of $a = 1.4$ microns, started off at radial distance of $r = 4 AU$. After 10^6 years, it moved to $r = 39.955 AU$. These little movements were already evident from figure 5.3. The sizes of the particles after settling with $\tau_{disk} = 10^6$ years, at $r = 40 AU$, were still micron sized. The Stokes numbers of micron sized particles at that particular radial distance, yields Stokes numbers with orders of about 10. This means that the particles are severely coupled to the gas and practically move along with the gas. The particles are too small to deviate in any way from the gas. Using figure 5.3, particles with Stokes numbers of order 10^{-5}, at $r = 40 AU$ have radial velocities of about $0.0021 \frac{m}{s}$. These radial movements are slow and larger particles are required for more radial movements.

When highlighting particles which do radially move, the particle starting from $r = 5 AU$ has a radius of $a = 730$ microns. After about 250000 years, it was able to drift and end up at $r = 0$. The particle itself has a local Stokes number of about 0.0058 which translates to a radial velocity at $r = 5 AU$ of about $5.8 \frac{m}{s}$. In this case, the particle moved about $5 AU$ in about 250000 years.

Movement for the turbulent scenario

Figure 5.5b visualises the radial movement of the largest particle per radius and it can be seen that radial drift does take place. Particles are able to drift radially by the diagonal lines. The largest particle at 50AU drifted to 20AU after 10^6 years. The drift from these particles is larger than the drift from the particles from the standard scenario. This is because the particles are larger than the ones from the standard scenario. The largest particle at 50AU for the standard scenario was

Furthermore, it can be seen that there are particles with smaller radial drift than particles from a farther radial distance. This is for instance the particle at .. AU. This is because of the particles resulting from the turbulent model. In the turbulent model, the largest particle turned into the largest particle by encountering nearly all other particles. This means that there is a single large particle per radial distance. However, there are also radii where there are several relative large particles, each having grown from the other particles. This means that there is no single large particle which has eaten nearly all other particles, but several relative large particles which have eaten nearly all particles in the radius. These are seen as the lines which radially drift at a slower pace.

5.3.1. Radial behaviours

What can be seen from theses results is that 1) small particles are not efficient in moving radially, and 2) moving radially is improved when located in low radial distances.

1 Small particles (from the standard case) are not efficient in moving radially as they are tightly coupled to the gas. This is evident via their small Stokes numbers of

orders of 10^{-5}. When particles are tightly coupled to the gas, their movements are completely dominated by the gas and are not able to deviate. Any deviation in movement of the particle w.r.t. the gas, due to for instance turbulence, will be completely gone soon as their the friction timescale will be low as well. This results in the fact that small particles only move along with the gas and thus, do not move radially;

2 When the particle is located in lower radial distances, the radial movement is improved. This was already evident from figure 5.3 where the largest radial velocities are obtained at lower radial distances. Furthermore, the radial movement is increased at lower radial distances as most particles are larger. It was mentioned in the previous chapter that larger particles are made due to settling at lower radial distances.

Particle density

As particles are moving inwards due to the radial movement, mass is moved from one place to another, changing the surface densities of disk. The changing surface density on the midplane is given in figure 5.5 for the standard scenario, and figure 5.6 for the turbulent case.

Figure 5.5 and 5.6 show plots at different times for the particle surface densities. The distribution of particle density only changes as the particles radially drift from one radius to another.

- For the standard case, the density distribution in higher radial distance regions is not changing with time due to the absence of radial drift from the particles as seen in figure 5.5. The density in the outer regions do not change as particles do not move radially. In the inner region, some changes in surface density can be observed. The radial velocity in the inner regions is larger as the particles in the inner region are larger. The larger inner particles are able to radially drift;

- For the turbulent scenario, changes can be observed. It can be seen that at the particle surface density changes. In the inner region, many particles are able to radially drift and drift into the central star. This is the reason why the inner region loses a portion of the initial surface density. Also, particles are able to radially drift from the outer region as the distribution changes. Lastly, the surface density at 50AU only decreases as there is no income of particles for that specific radius.

5.4. Mass flux

The mass flux is the mass of the particles passing per unit of time. The mass flux of particles is required for the pebble accretion calculations in chapter 6. During the calculation of planet growth, the gain in mass originates from the mass flux from the pebbles and the mass flux is calculated in this section. The mass flux is calculated as [16]:

$$\dot{M}_p(t) = 2\pi r v_r \Sigma_p \tag{5.13}$$

Where r is the radial distance, v_r is the radial velocity and Σ_p is the particle surface density. For each particle, the radial velocity is found from figure 5.4, and the respective

(a) Particle density at t = 0 years

(b) Particle density at t = 200000 years

(c) Particle density at t = 400000 years

(d) Particle density at t = 600000 years

(e) Particle density at t = 800000 years

(f) Particle density at t = 1000000 years
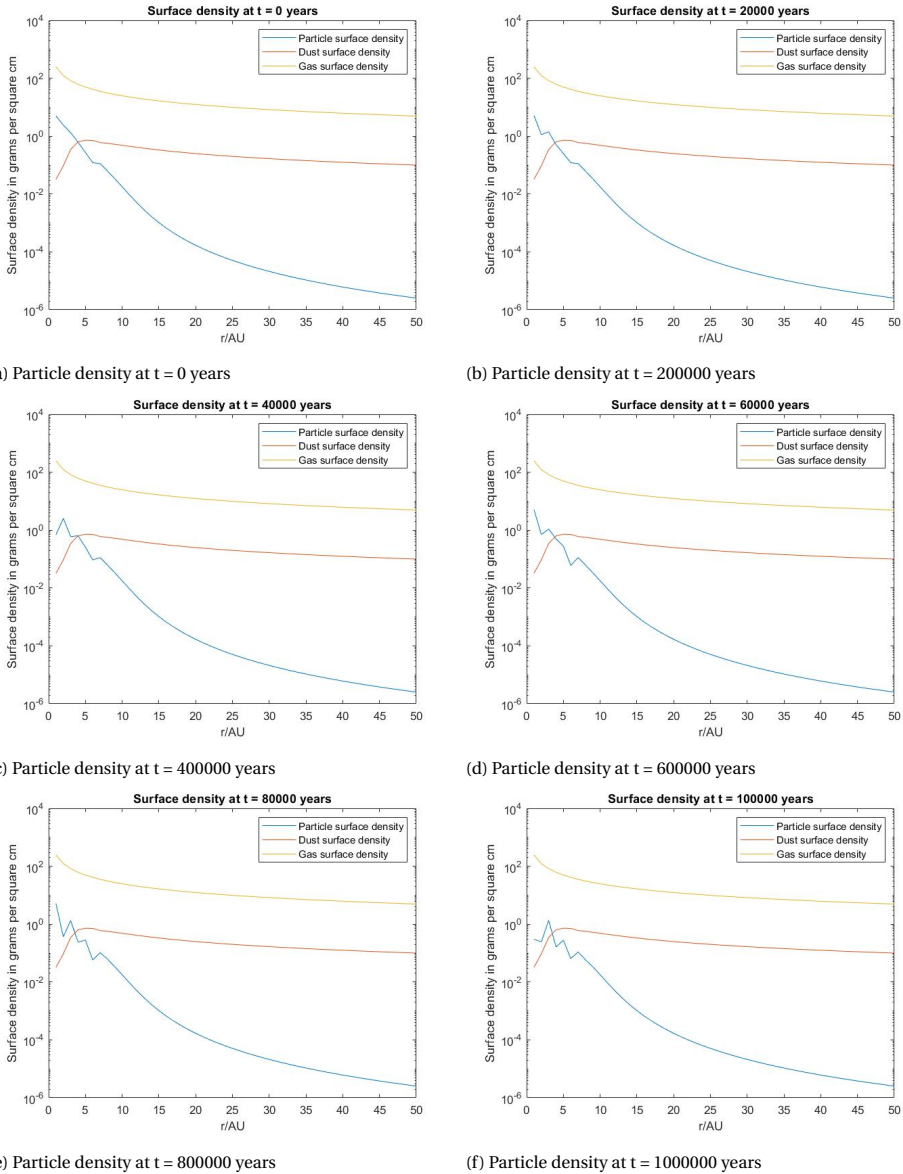
Figure 5.5: The density distribution of the particles over the radial distance for the standard scenario. The line represents the density of particles. Each panel represents the density distribution at a specific time.

surface density of that specific particle is used. Then, the mass flux is calculated for that specific particle, and the total massflux per radial distance is calculated for each radial distance. The mass flux over radial distance for the standard case is then given in figure 5.7, and the mass flux for the turbulent case is given in figure 5.8.

(a) Particle density at t = 0 years

(b) Particle density at t = 200000 years

(c) Particle density at t = 400000 years

(d) Particle density at t = 600000 years

(e) Particle density at t = 800000 years

(f) Particle density at t = 1000000 years
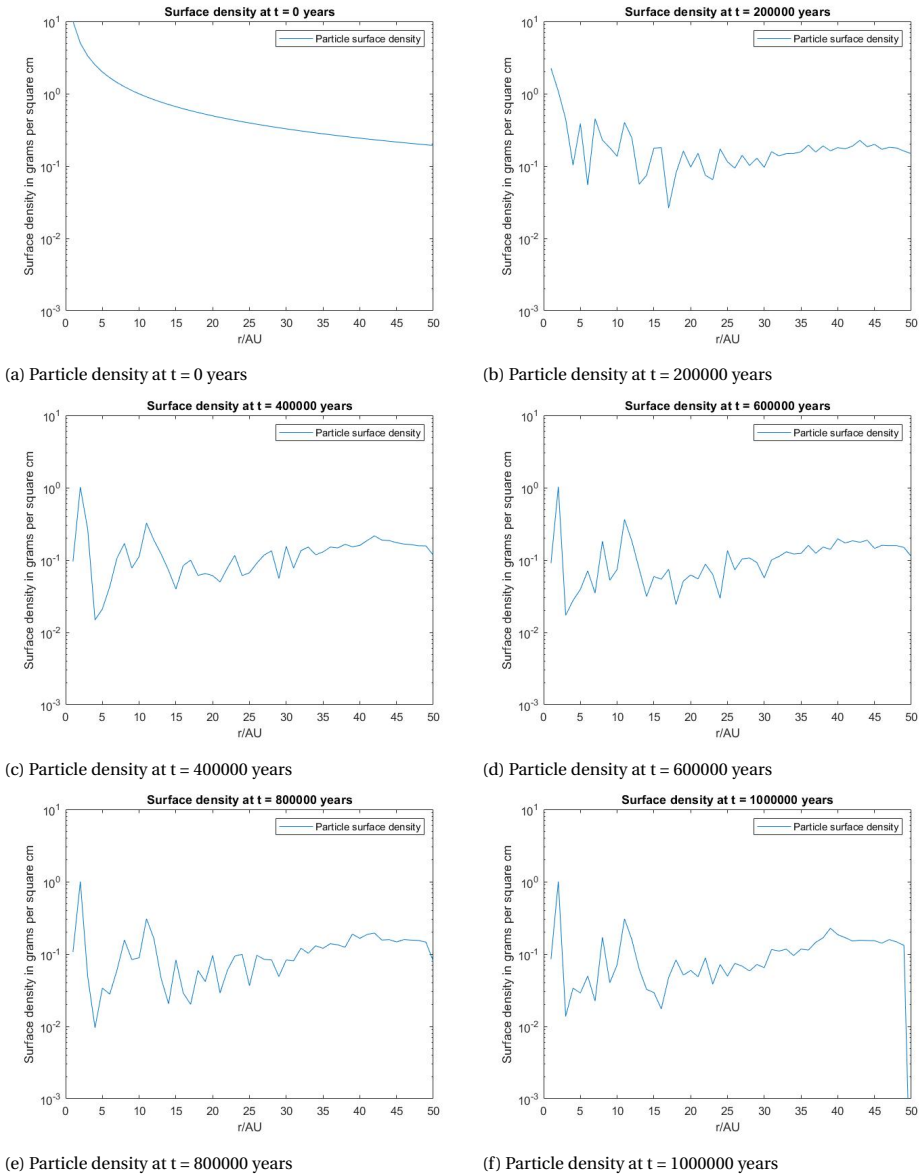
Figure 5.6: The density distribution of the particles over the radial distance for the turbulent case.. The line represents the density of particles. Each panel represents the density distribution at a specific time.

As seen in figure 5.7, there is little change in the mass flux for the standard model and lots of more changes in the turbulent model. This is expected based on the behaviour of the radial drift.

is larger near the central star and small farther away. As the mass flux is calculated

(a) Mass flux at t = 0 years

(b) Mass flux at t = 20000 years

(c) Mass flux at t = 40000 years

(d) Mass flux at t = 60000 years

(e) Mass flux at t = 80000 years

(f) Mass flux at t = 100000 years
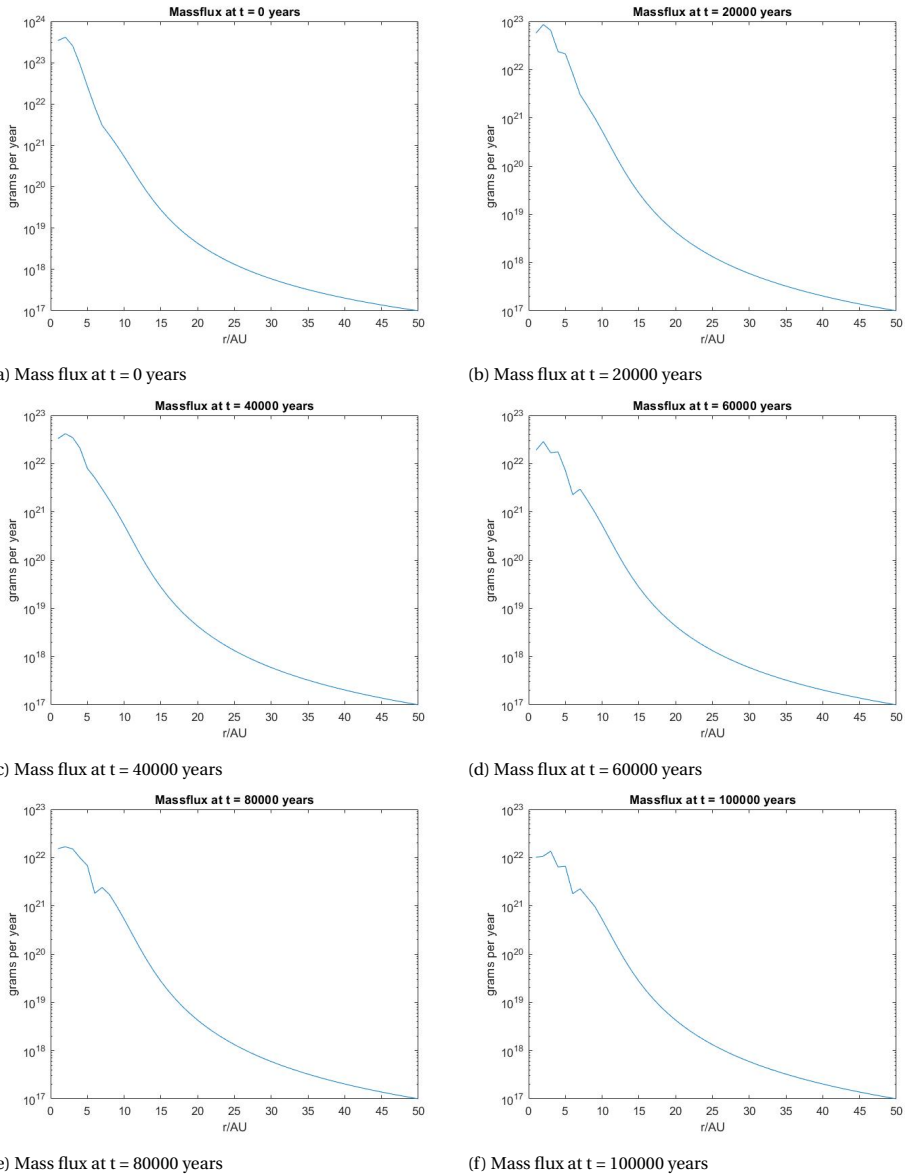
Figure 5.7: The mass fluxes for the standard model. Each panel represents a different time, and the figure are shown from $t = 0$ up to $t = 10^6$ with intervals of 200000 years.

according to equation 5.13, it is dependent on the radial velocity, radial distance and surface density of the particles.

- The mass flux for the standard model is larger near the central star due to the larger particle density near the central star. From figure 5.5, the particles at $r = 1$AU are

(a) Mass flux at t = 0 years

(b) Mass flux at t = 200000 years

(c) Mass flux at t = 400000 years

(d) Mass flux at t = 600000 years

(e) Mass flux at t = 800000 years

(f) Mass flux at t = 1000000 years
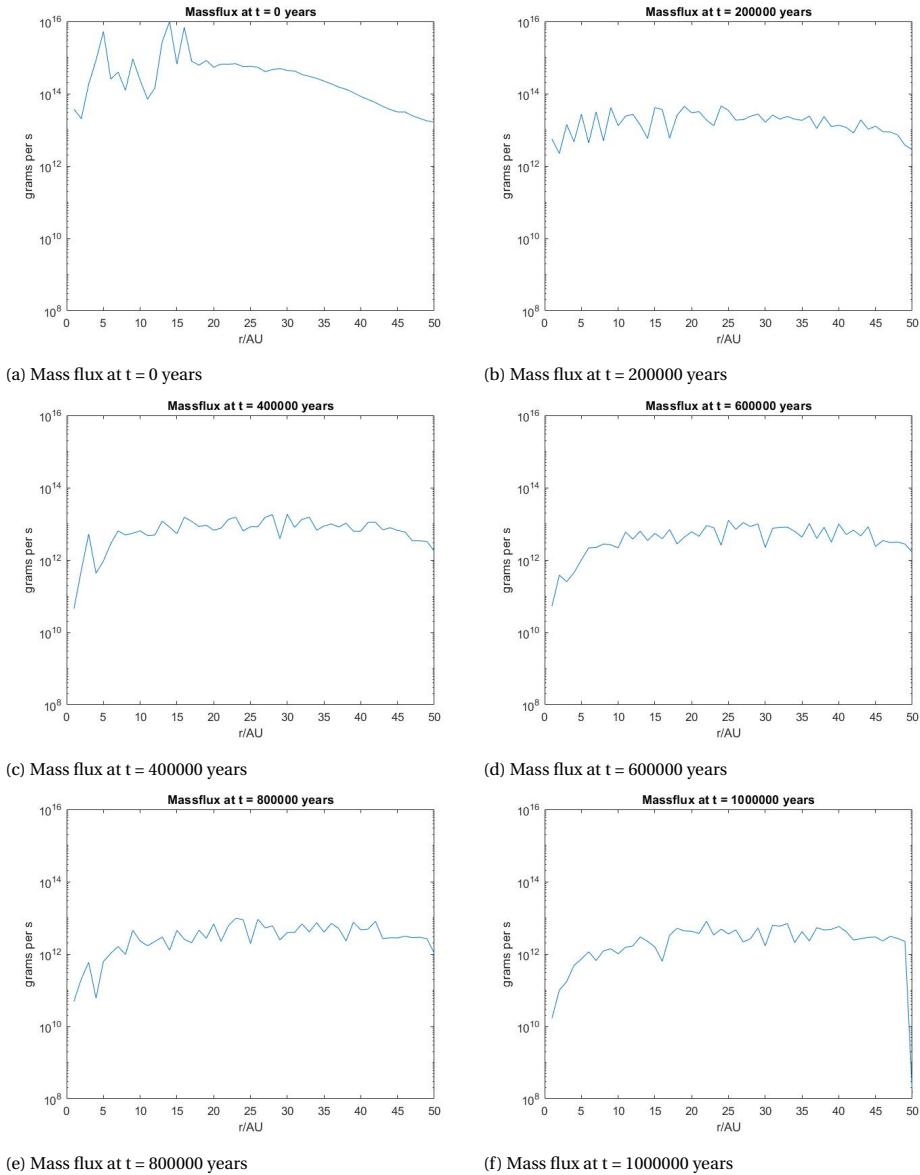
Figure 5.8: The mass fluxes for the turbulent model. Each panel represents a different time, and the figure are shown from $t = 0$ up to $t = 10^6$ with intervals of 200000 years.

an order of 10^4 larger than the ones from $R = 30$AU, which translates into a larger mass flux at those close regions;

- The mass flux increases with increasing radial distance. If only based on the radial distance, the mass flux at $r = 50$AU would be 50 times larger than the mass flux

at $r = 1$AU. However, the decrease of mass flux resulting from the surface density, results in larger mass flux at low radial distances, and smaller mass flux at high radial distances;

- The radial velocity is dependent on the local gas density, and the sizes of the particles. These two parameters are incorporated in the Stokes number. Generally, the Stokes numbers of particles are larger than the Stokes numbers of particles farther away due to the larger sizes. This translates to higher radial velocities as seen in figure 5.3 and results in larger mass fluxes at lower radial distances than higher distances;

- For the turbulent case, the initial mass flux is largest. The difference between the first panel a) and second panel b) is large compared to the difference between panel c) and d) or any other panel. This is due to the radial drift of the largest particles which takes place only in the very first few years. That is when the largest particles radially drift into the star and the inner region loses mass. This can be seen as the first panel a) included mass fluxes of orders of 10^16 grams per second and the others go up to orders 10^13. The remaining mass consist of other particles which radially drift at a slower pace and that is seen by the small changes between the panels other than panel a).

6

PLANET FORMATION

With the results from chapter 4 and 5, the building blocks for planet formation using the pebble accretion are laid. In this chapter, focus is given on the formation of planets from a planet seed, which will grow via pebble accretion. The pebble accretion process is detailed, and performed with the available pebbles created in the previous chapters. From the last chapters, the formation of pebbles when the disk is subjected to strong gas decay or in presence of turbulence was computed. These two scenarios provided different distribution of pebbles within the disk. In the present chapter, the formation of planets with pebbles formed via these two scenarios is also studied.

6.1. PEBBLE ACCRETION AND REGIMES

It is established that there are large amounts of pebbles in the PPD present among planet cores and planetesimals. This is a strong motivation to consider pebbles as the building blocks for planets. Simulations [22] show that rapid accretion rates are possible when protoplanets accrete pebbles of different sizes. For this reason, pebble accretion is considered as a potential theory for planet formation. Pebble accretion is a planet formation concept which involves the accretion of small pebbles onto larger bodies. The small pebbles are considered to have negligible mass, compared to the larger mass. This means that the pebble is considered aerodynamically small and the larger body is considered gravitationally large.

Aerodynamically small pebbles have Stokes numbers $0.001 < \tau_s < 1$. Gravitationally large bodies are masses which have Stokes numbers $\tau_s >> 1$. [3]

Pebble accretion is able to achieve high accretion rates of pebbles because of drag forces exerted by the gas on the pebbles in the PPD. The drag allows for scattering process of pebbles passing a growing planet seed. There are two regimes in pebble accretion, which are described as the *Bondi regime* and the *Hill regime*. These are separated by a transition mass of a planet:

$$M_t = \sqrt{\frac{1}{3}} \frac{\Delta v^3}{G\Omega} \tag{6.1}$$

Where Δv is the sub-Keplerian speed, G is the gravitational constant, and Ω is the orbital frequency.

Bodies with masses smaller than the transition mass are in the Bondi regime. The interaction radius between core and pebbles is given as the Bondi radius:

$$R_B = \frac{GM_c}{\Delta v^2} \tag{6.2}$$

Where M_c is the mass of the core. Pebbles approaching the core within this radius with relative velocity Δv get deflected [23]. In this regime, pebbles approach the core with sub-Keplerian speeds Δv and the interaction between the pebble and the core is set by the friction timescale t_f relative to the timescale for the pebble to pass the core $t_B = R_B/\Delta v$. Pebbles with Stokes numbers $\tau_s > 1$ have large friction timescales, and are scattered by the core. Pebbles with Stokes numbers $0.001 < \tau_s < 1$ have friction timescales similar to the t_B and are accreted within the Bondi radius. Particles with Stokes numbers $\tau_s < 0.001$ have very short friction timescales compared to t_B and are only accreted from shorter impact parameters. If too large, the pebble is coupled to the gas and will only be scattered by the protoplanet. These interactions are visualised in figure 6.1a.

However, the growth of a core within the Bondi regime is not sustained. Once the mass of the planet reaches the transition mass M_t from equation 6.1, it enters the Hill regime and Hill accretion will occur.

Bodies with masses larger than the transition mass are in the Hill regime. The interaction radius between core and pebbles is given as the Hill radius:

$$R_H = \left(\frac{GM_c}{3\Omega^2}\right)^{\frac{1}{3}} \tag{6.3}$$

In this regime, pebbles approach the core with Hill speed $v_H = R_H\Omega$. The interaction between pebble and core is again set by the friction timescale t_f relative to the characteristic timescale for the pebble to pass the core, which is in this case: $t_H = R_H/v_H = \Omega^{-1}$. It can be seen that t_H is independent of the mass of the core and accretion is fully determined by the friction timescales or Stokes numbers. Pebbles with large Stokes numbers $\tau_s > 1$ are scattered again, but pebbles with smaller Stokes numbers $\tau_s < 1$ are accreted. These interactions are visualised in figure 6.1b.

6.2. CORE GROWTH
In this chapter, only the Hill accretion is considered for the reason that the Bondi accretion is not sustained and will transition into the Hill accretion once the core reaches the transition mass. A planet core is assumed to be present to grow from pebbles, and

(a) Interactions of pebbles with the planetcore in the Bondi regime. The blue lines are pebbles with large Stokes numbers and are scattered. The red lines are pebbles with optimal Stokes numbers and are accreted. The orange lines are pebbles with small Stokes numbers and only the ones close to the core are accreted.

(b) Interactions of pebbles with the planetcore in the Hill regime. The blue lines represent pebbles with large Stokes numbers and are scattered. The red lines are pebbles with optimal Stokes numbers and are accreted. The orange lines are pebbles with small Stokes numbers and are also accreted by the core.

Figure 6.1: The interactions of particles with Stokes numbers in both the Bondi regime (left) and the Hill regime (Right). Taken from Lambrechts et al. [24].

the transition mass is used as the initial cores mass, calculated using equation 6.1. The growth of the core in the Hill regime is given as [25]:

$$\dot{M}_c = 2 r_H \Sigma_p v_H \tag{6.4}$$

Where Σ_p is the surface density of pebbles, v_H is the Hill speed of the approaching pebble, r_H is the Hill radius of the core. The available pebble surface density is calculated in the previous chapter.

SIMULATION

The simulation for the core growth starts off with five planet cores with mass m_t at the locations: 1AU, 5AU, 10AU, 19AU, and 30AU. These are the respective locations of Earth, Jupiter, Saturn, Uranus and Neptune. Each core starts with an initial mass, which is the transition mass calculated using equation 6.1. The transition mass is calculated to be: 0.01 Earth masses and are constant for each planet. This is because of transition mass m_t, which is proportional to Δv^3 and inversely proportional to Ω. As both of these parameters grow proportional to $\sqrt{\frac{1}{r^3}}$, the transition mass is constant for each radius. Figure 6.2 visualises the transition mass from equation 6.1.

Using the initial masses at each location, the planet cores grow using equation 6.4 over a period of 10^6 years and with timesteps dt of 1000 years. The planet core grows mass dm each timestep, and the growth is dependent on the Hill radius r_H, the Hill speed $v_H = r_H \Omega$, and the pebble surface density Σ_p. The pebble surface density Σ_p is retrieved from chapter 5 and consists of matrices with the evolution of the pebble surface densities over a period of 10^6 years.
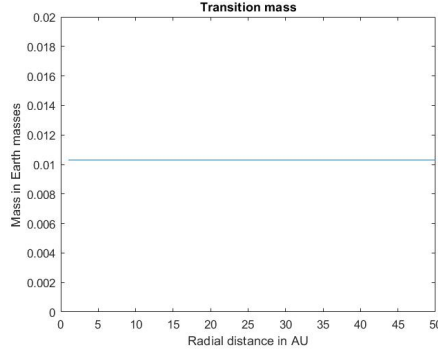
Figure 6.2: The transition masses from equation 6.1 calculated at each radial distance. The masses are constant as the transition mass is inversely proportional to Ω and proportional to Δv^3. Δv^3 is the difference in the rotational gas velocity and the Keplerian velocity. Both Ω and Δv^3 are proportional to $\sqrt{\frac{1}{r^3}}$, which results in the constant transition masses for each radius.

The decrease in pebble density due to the growth of the core is regulated using the mass flux, which was also calculated in chapter 5. The mass flux encapsulates the available incoming mass per time unit at a specific radial distance. This is also the total available mass for a planet to grow from per time unit at a specific radius. In this case, the increase in mass per time unit for the planet is a decrease in mass flux of the pebbles $\dot{M}_p$. The decrease in mass flux can be translated again in a decrease in pebble surface density. This way, the available mass is conserved. The change in mass flux is calculated as:

$$\dot{M}_{p\,i+1} = \dot{M}_{p\,i} - \dot{M}_c \tag{6.5}$$

Where subscript i represent the timesteps. The mass flux from equation 6.5 is the mass which has not been accreted by the planet and will continue to move radially. The surface density for this mass flux is then calculated as:

$$\Sigma_{p_{i+1}} = \frac{\dot{M}_{p_{i+1}}}{2\pi r\, v_r} \tag{6.6}$$

6.3. RESULTS
In this section, planets formed from equation 6.4 are discussed. From the previous chapters, three different particle growth scenarios were detailed. Each growth scenario resulted in different pebble surface density distributions and evolutions. The growth of these cores differ as a result from these different distributions and evolutions. Each growth scenario is detailed subsections.

6.3.1. STANDARD SETTLING AND COAGULATION MODEL
The growth of the planet cores is dependent on the pebbles formed from standard settling, coagulation and radial drift at the local radial distance. In figure 6.3, the surface

densities of pebbles are visualised.
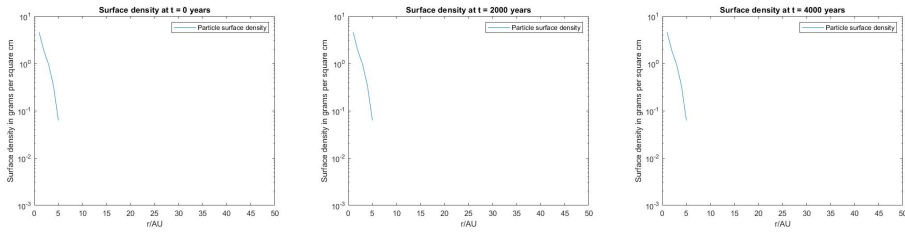
(a) The pebble surface density at t = 0 years

(b) The pebble surface density at t = 2000 years

(c) The pebble surface density at t = 4000 years
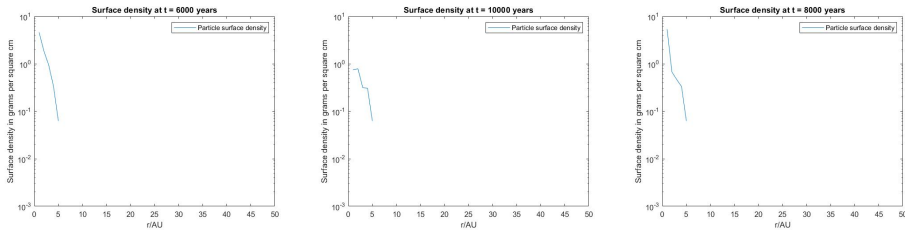
(d) The pebble surface density at t = 6000 years

(e) The pebble surface density at t = 8000 years

(f) The pebble surface density at t = 10000 years
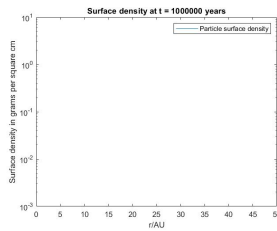
(g) The pebble surface density at t = 1000000 years

Figure 6.3: The pebble surface density from particles which grew via settling and coagulation. The upper six panels (a-f) represent times between $0 - 10^4$ years. The last panel (g) represents the final time at 10^6 years. It can be observed that pebbles are only present in the inner regions in the earlier years and are depleted in the later years.

Each panel in figure 6.3 visualises the pebble surface density at a specific time. The upper six panels represent times $0 - 10^4$ years and the seventh panel represents the final time of 10^6 years. It can be seen that there are only pebbles in the inner region and no pebbles in the outer region. Furthermore, there are no more pebbles at later times as pebbles have radially drifted into the star. This is the reason for the lack of pebbles in the panel representing $t = 10^6$ years.

Figure 6.4 visualises the growth of each core. Each line represent the mass of the core over time and it can be seen that the cores do not form planets. The largest planet core is able to grow up 0.3 Earth masses. The lack of growth for the cores is due to the small amount of pebbles, as shown in figure 6.3. As stated, pebbles were only present in the earlier years, and only in the inner regions. This is reflected in the growth, as only the
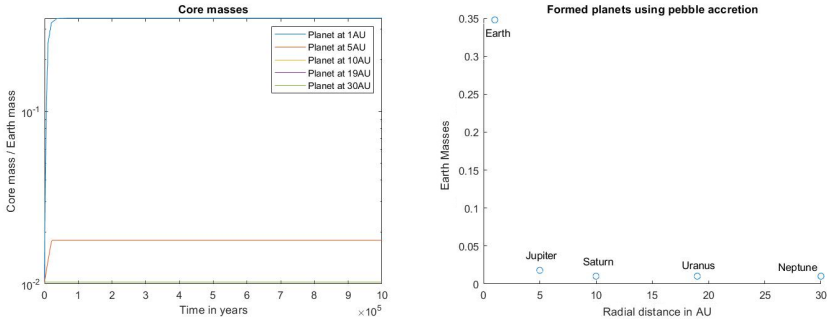
(a) The growth of seed cores. Each line represents a the (b) The final masses of the planets grown. The final time mass of a core at different radii. The growth of each core of the simulation is 10^6 years. Each dot represents a is simulated for 10^6 years. planet seed at the location the named planet.

Figure 6.4: The growth of the planet seed (left) and the final masses of the grown planets(right).

inner two planet cores grew in size, and all other cores did not. After some time, the pebbles were depleted from the growth and the radial drift and the cores were not able to grow.

6.3.2. GAS DECAY MODEL

There are no planets formed using the pebble distribution resulting from the gas decay scenario. This is the result of the dissipated gas density. With the low gas density, the Stokes numbers of the particles increased into orders of 10^6; the particles became de-coupled from the little gas that is left. This means that all particles in the disk are not pebbles as their Stokes number are not in the $\tau_s = 1 - 10^{-3}$ [−] criterion. The cores will not able to grow as there are no pebbles, and no planets are formed.

6.3.3. RESULTS FOR TURBULENT SCENARIO

Planets formed using the pebbles resulting from the turbulent growth scenario is discussed in this subsection. In this scenario, particles were able to reach larger sizes and become pebbles. The surface density of pebbles is given in figure 6.5. Figure 6.5 visualises the surface density of pebbles over time as they move radially. Each panel represents the surface density at a different time. The upper six figures represent the surface density at 0 to 10^4 years, and the last panel represent the surface density at 10^6 years. The surface density at 10^6 is lower than the earlier years, as most pebbles have moved radially and or into the central star. Also, it can be seen in the earlier years ($0 - 10^4$ years), that there are more pebbles in the inner regions, while at 10^6 years, the pebble surface density in the inner region is lower than the pebble surface density in the farther regions. The reason for this effect is that the pebbles will move radially and eventually into the star. Pebbles from outer regions will also radially drift inwards. However, a pebble in the outer regions might not be a pebble in the inner region. This is due to the larger gas density in the inner region. The gas density decreases over increasing radial distance and as the Stokes number is inversely dependent on the gas density, the Stokes number will decrease with increasing density (the gas experienced increases as the particle radially

(a) The pebble surface density at t = 0 years

(b) The pebble surface density at t = 2000 years

(c) The pebble surface density at t = 4000 years

(d) The pebble surface density at t = 6000 years

(e) The pebble surface density at t = 8000 years

(f) The pebble surface density at t = 10000 years

(g) The pebble surface density at t = 1000000 years
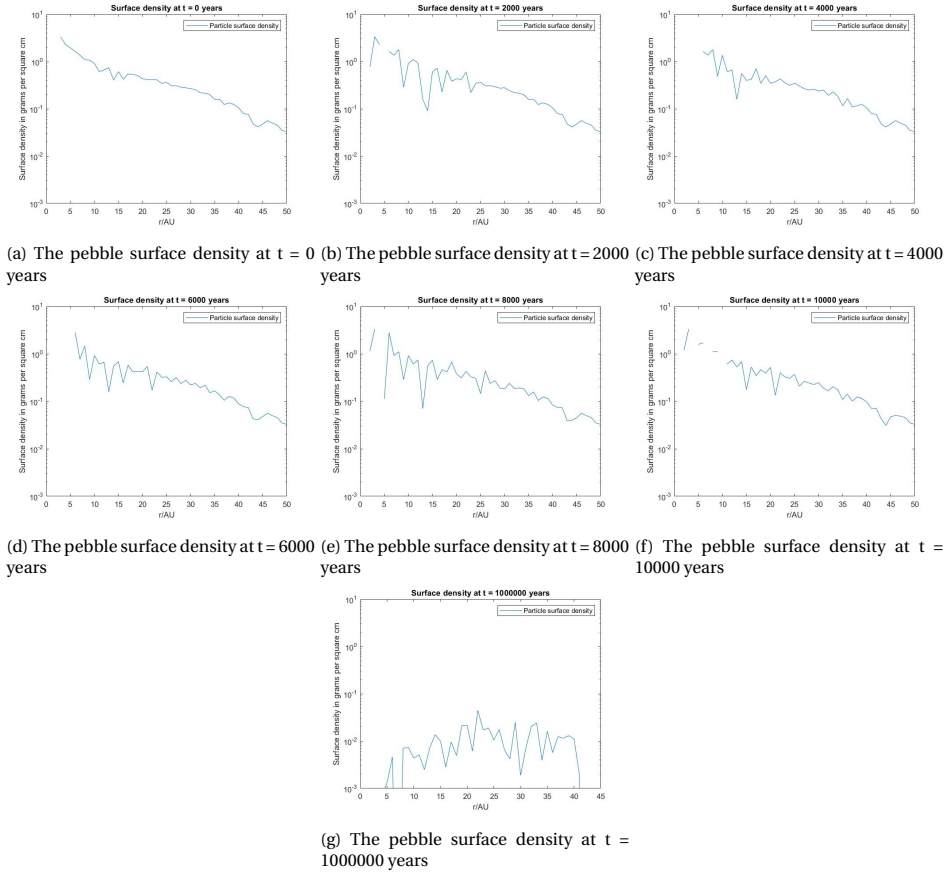
Figure 6.5: The pebble surface density from particles which grew via turbulence. The upper six panels (a-f) represent times between 0010^4 years. The last panel (g) represents the final time at 10^6 years. It can be seen that pebbles deplete in the inner region over time while the outer regions will contain pebbles until the final time.

drifts inwards). If the smaller pebbles from farther regions would end up in the inner regions (due to radial drift), the larger gas density in that region might cause the Stokes number of that pebble to fall out of Ormel's limit of between 1 and 10^{-3}. If this happens, a pebble in farther regions will not be a pebble in the inner region. Replenishment of pebbles in the inner region occurs little and is the cause of the decrease in pebble as seen in figure 6.5.

Using equation 6.4, planets cores grow at the earlier mentioned radial locations of 1AU, 5AU, 10AU, 19AU, and 30AU. The growth of these cores is given in figure 6.6.

- At 1 AU, the planet seed is able to grow into a mass of about 0.05 Earth masses. The main reason for the small planet is due to the depletion of pebbles which radially drift inwards and drift away into the central star. Also, no pebbles are replenished in this region pebbles as pebbles in farther regions might not be pebbles in the
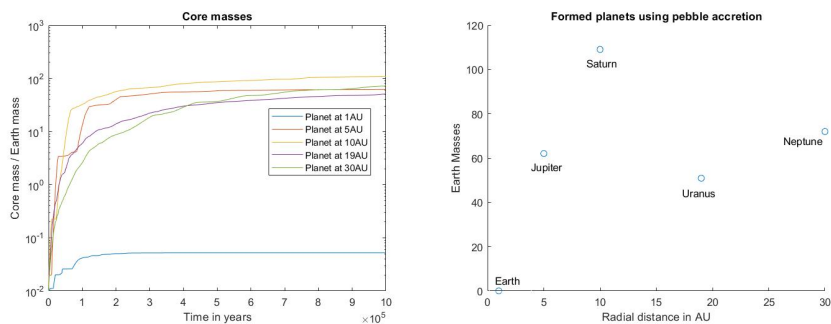
(a) The growth of seed cores. Each line represents a the mass of a core at different radii. The growth of each core is simulated for 10^6 years.

(b) The final masses of the planets grown. The final time is 10^6 years. Each dot represents a planet seed at the location the named planet.

Figure 6.6: The growth of the planet seed (left) and the final masses of the grown planets (right).

inner regions due larger gas density in the inner region;

- At farther distances, the planets are able to grow into larger sizes. The planet at 10AU is able to grow into 200 Earth masses, and the other planets are able to grow into about $50-70$ Earth masses. The planet cores are able to grow into larger planets than the one from 1AU is due to the fact that there are more pebbles in these regions. In these regions, the smaller gas density allows for the particles to have Stokes numbers within the criterion of 1 and 10^{-3}. This means that there are more pebbles present in farther regions which are available for the planets to grow from.

6.4. SUMMARY OF RESULTS

From the standard scenario with settling and coagulations, no planets are formed as there were no pebbles for the planets to grow from. The turbulent scenario resulted in planets and larger planets were found in the outer regions. The gas density in the outer region allowed for more particles to become pebbles, from which the planets were able to grow from. Figure 6.7 visualises the results found for the two scenarios. The blue dots represent the planets from the turbulent model and the orange dots represent the planets from the standard model. The height and size of the dots represent the masses of the planets.

Figure 6.8 is given for a comparison between the results from the turbulent simulation and the planets in our Solar system. The Earth and Jupiter formed from the turbulent model are smaller than the actual planets. Uranus and Neptune formed from the model are larger than the actual planets. This shows a growth favouring planets in the outer region and is the result of the larger presence of pebbles in the outer region. Solutions to these deviations are proposed in the discussion section in this chapter.
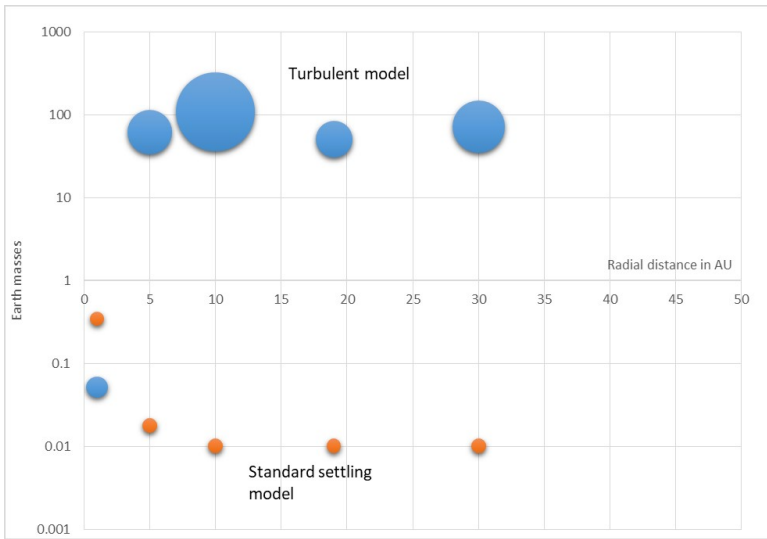
Figure 6.7: The planets formed from the standard settling model and the turbulent model. The blue dots represent the planets formed from the turbulent model, and the orange dots represent the planets found from the standard model and the height and size of the dots represent the masses of the planets.
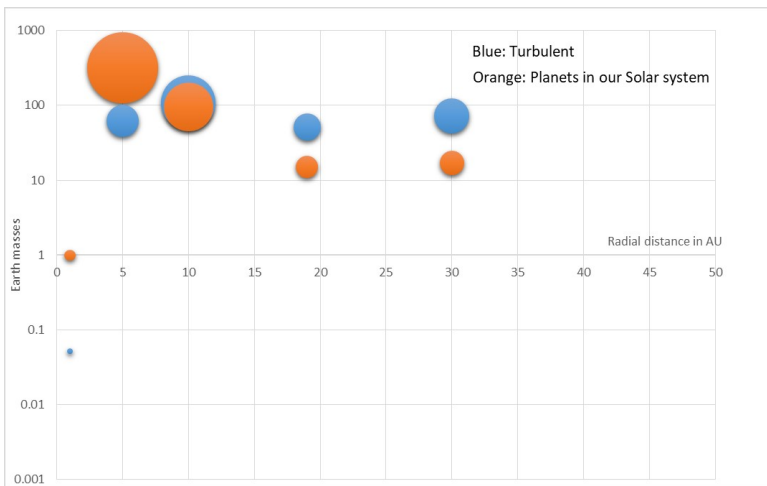
Figure 6.8: The planets formed from the turbulent model and the actual planets in our Solar System. The blue dots represent the planets formed from the turbulent model, and the orange dots represent the actual planets and the height and size of the dots represent the masses of the planets.

6.5. COMPARISON WITH LITERATURE

In this section, a comparison with results from Lambrechts and Johansen [16] is made. In their research, planet formation using pebble accretion was investigated. From a growth model using turbulence to grow dust into radially drifting pebbles of radius $1-10$mm,

the pebble surface densities is visualised in figure 6.9. As a reference the pebble surface density from the turbulent case in this thesis is also given.
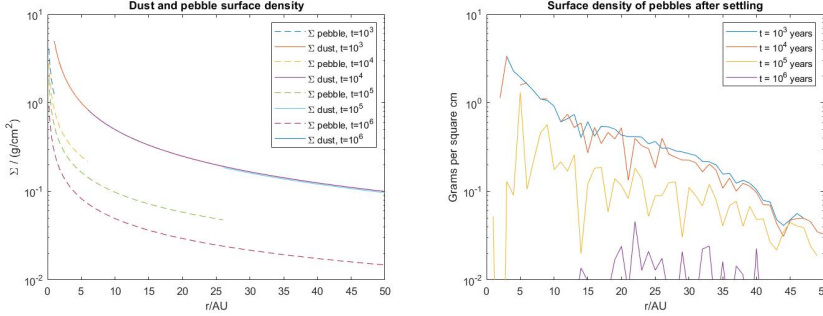
(a) The pebble surface density calculated by Lambrecht et al. [16].

(b) The pebble surface density calculated in this thesis after settling using the turbulent case.

Figure 6.9: Left) the surface densities of Lambrechts et al. [16] and right) the surface density from this thesis. For the left hand panel, the dotted lines represent the pebble surface densities at a specific time, and the solid lines represent the dust densities.

The surface density from the literature is calculated according to an assumption that particles with a certain radius of 1mm - 10mm are considered pebbles and are able to radially drift. With this assumption, the time required for a particle to grow from ISM sizes of 1 micron into this size is calculated using:

$$t_{g,peb} = \frac{4}{\sqrt{3}\epsilon_d \left(\Sigma_d/\Sigma_g\right)\Omega} \tag{6.7}$$

Where ϵ_d is the coagulation efficiency. Rewriting this equation to solve for the radius r in the orbital frequency Ω leads to:

$$r_g = \frac{3}{16}^{1/3} (GM)^{1/3} \left(\epsilon_d \Sigma_d/\Sigma_g\right)^{2/3} t^{2/3} \tag{6.8}$$

This is called the pebble production line and defines the radius at which pebbles are incoming from outer radii. This also means that all pebbles originate from regions outside of the pebble production line and the existing particles inside of the pebble production line are not considered. At the pebble production line, pebbles are incoming, which were originally dust particles outside of the pebble production line. The incoming mass flux is then given as:

$$\dot{M} = 2\pi r_g \frac{dr_g}{dt}\Sigma_{dust}\left(r_g\right) \tag{6.9}$$

The pebble mass flux inside of the pebble production line is defined as.:

$$\dot{M} = 2\pi r\Sigma_p v_r \tag{6.10}$$

Using continuity: filling in equation 6.9 into 6.10, and using radial velocity: $v_r = -2\tau_s\eta v_k$ and the Stokes number: $\tau_s = \frac{\sqrt{3}\epsilon_p\Sigma_p}{8\eta\Sigma_g}$, the surface density of pebbles can be cal-

culated as:

$$\Sigma_p = \sqrt{\frac{2\dot{M}_p \Sigma_g}{\sqrt{3}\pi \epsilon_p r \nu_k}} \tag{6.11}$$

Where ϵ_p is the coagulation efficiency of pebbles. The surface density of pebbles is defined by the incoming dust density at the pebble production line. The pebble production line changes over time and is in figure 6.9 indicated as the transition between the dotted and the solid lines.

The total mass $(\Sigma_d + \Sigma_p)$ in this calculation is not conserved as the calculations of the pebble surface densities is based on the surface densities at the pebble production line. This means that the surface densities inside of the pebble production line are based on pebbles which arrived from the pebble production line. The original particles and or pebbles present were not considered. This can be seen as the gap between the dotted lines and the solid lines. The surface densities are lower than the ones calculated in this thesis.

The planets obtained from these pebbles using transition masses are visualised in figure 6.10 along with the planets obtained in this thesis using the turbulent model:
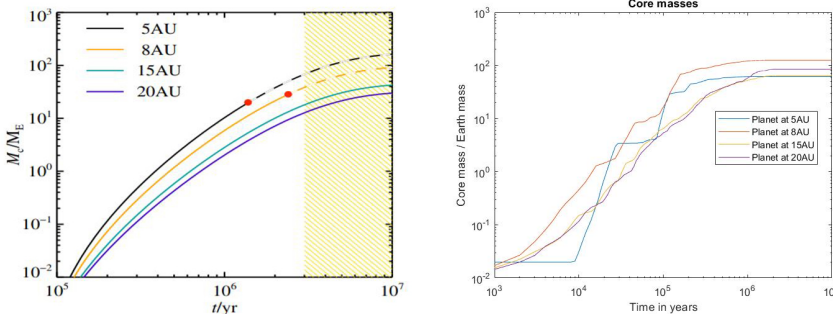
(a) The planets calculated by Lambrecht et al. from the pebbles in figure 6.9 [16].

(b) The planets calculated from this thesis using the turbulent case

Figure 6.10: The planets calculated by Lambrechts et al. [16] and the planets from this thesis. The red dots in the right hand figure represent the critical mass at which the gas accretion initiates. The yellow region in the left hand figure represents the time at which the gas has dissipated from the disk.

The left hand figure represents the results from Lambrechts et al. [16] and the right hand figure represent the planets found using the turbulent case in this thesis. From observing the figures the following points can be found:

- The final masses of the planets in both simulations are similar as the planets at 5 and 8AU are able to reach masses near the 100 Earth mass;

- The growth time takes longer in Lambrechts et al. case. After 10^6 years, the planet at 5AU has a mass of about 30 Earth masses while in the simulation from this thesis, the planet has a mass of about 100 Earth masses.

Next, some key differences are highlighted:

- The differences in pebble surface densities result in the differences in planets formed. One can already observe that the pebble surface densities from the literature are lower than the ones calculated in this thesis. When growing the particles using equation 6.7, the growth efficiency factor was used and set to 0.5. While in this thesis no efficiency factor was used for the growth during settling. This has a major impact on the surface densities;

- Another difference in pebble surface density lies in the calculations of the literature where it is assumed that pebbles only originate from outside the pebble production line. The calculations for the pebble surface density inside of the pebble production line is based on the incoming pebbles from the pebble production line. This means that existing particles or pebbles inside of the pebble production line are not taken into the calculations;

- In the literature, growth of pebbles or particles was still present during radial drift. This is evident in equation 6.7 and the radial drift. The calculation of the Stokes number: $\tau_s = \frac{\sqrt{3}\epsilon_p \Sigma_p}{8\eta \Sigma_g}$ was based equating equation 6.7 with the radial velocity. As the particles were growing, the radial drift in the literature is more efficient than the radial drift in this thesis. The pebbles would be replenished faster in the literature. However, this is difficult to observe as the growth efficiency factor resulted in less pebbles in the first place.

6

6.6. DISCUSSION

6.6.1. THE STOKES NUMBER PARAMETER

The Stokes numbers have large impact on the formation of planets using pebble accretion as pebbles are required for the planets to grow. Whether or not a particle is considered a pebble, is based on Ormels criterion which states that particles require Stokes numbers of between: $1 < \tau_s < 10^{-3}$ [−] (from now referred as Ormels criterion). The equation for the Stokes number is give again:

$$\tau_s = \frac{\rho_p a}{\rho_{gas} \bar{v}} \Omega$$

EFFECT OF THE GAS DENSITY ON THE STOKES NUMBER

The Stokes number is inversely dependent on the local gas density. If the gas density increases, the Stokes number decreases. For this reason, pebbles will only form in certain regions where the gas density allows the Stokes number to be within Ormels criterion. In case of the standard scenario with settling and coagulation, most of the particles were not pebbles as their Stokes numbers were too small. If the gas density were lower, it would allow for more pebbles as the Stokes numbers would increase.

This would mean that smaller disks with smaller gas density, would allow for more pebbles as the lower gas densities allows for particles to have larger Stokes numbers. However, this would also potentially result in less pebbles as there will be less material for the particles to grow from. The settling particles might end up with smaller radii and Stokes numbers would be small.

Lastly, gas decay would also allow for pebbles at a certain moment. As the gas decay continues, the gas density decreases and pebbles will form as well as the Stokes numbers of the particles increase. However, this is only temporary as eventually, the upper limit of Ormels criterion is met and particles are no more pebbles.

EFFECT OF THE RADIUS OF THE PARTICLE ON THE STOKES NUMBER

The particle radius is dependent on the Stokes number of that particle. If too small, the Stokes numbers would be too small, and if too large, the Stokes numbers would be too large. From the standard scenario, particles grew into sizes of a few hundred microns in radius which are too small to form enough pebbles for the planets to grow. For more efficient growth, combinations of effects is recommended which incorporates several growth sources. In the settling simulation in this thesis, growth was only performed during settling as a result of encounters with dust and other particles with a relative velocity which was either the settling velocity, Brownian velocity or the relative turbulent velocity. This means that the growth of the particle depended on one of the three velocities while in reality the growth of a particle would depend on all velocities. A model in which all three growth sources would be processed at coincidently would result in larger particles and reflect reality more closely.

6.6.2. THE SMALL EARTH IN THE TURBULENT CASE

Based on the results from the turbulent case, no Earth was formed. Figure 6.6 showed that the growth stagnates at around 2×10^5 years. In this case, the simulation only included a growth model using an initial planet core. No other effects are taken into account such as radial drift of planets or scattering of planetesimals as a result of interactions with planets. If taken into account, such as the "Grand Tack" model of Walsh [26], different results will come up. The Grand tack model is a model scenario which proposes that Jupiter and Saturn radially drifted inwards from their initial positions. Jupiter would radially drift inwards using type-I migration, and Saturn would radially drift type-II migration as it was smaller. As Saturn was drifting faster than Jupiter, the planet caught up with Jupiter and as the two planets met, the gaps around the two planets overlapped. Saturn's gap was not fully cleared, resulting in an outer edge of material. The planets experience a decrease of negative torque from the outer edge, which translates in an increase in net torque and the planet migrate outwards. This outwards movement lasts until the gas in the disk is fully dissipated. However, the inwards movement of the planets scattered many of the particles in the disk. Outer planetesimals are scattered inwards, allowing for planetesimals in the inner region to grow from the incoming particles. This is also simulated by Carter et al. [27] in which two terrestrial planet growth simulations were performed using n-body and collisional models. One simulation was performed incorporating the Grand Tack, while other simulation had no influence of the giant planets. In the Grand Tack scenario, outer planetesimals are scattered and inner planetesimals were able grow. The other simulations show little scattering of planetesimals as there was no influence of giant planets. This means that inner planets were not able to grow as efficiently as in the Grand Tack scenario because of the lack of incoming outer material. Results of this simulation are visualised in figure 6.11 In figure 6.11, two panels are shown of masses of planetesimals in over radial distance. The left panel visualises the
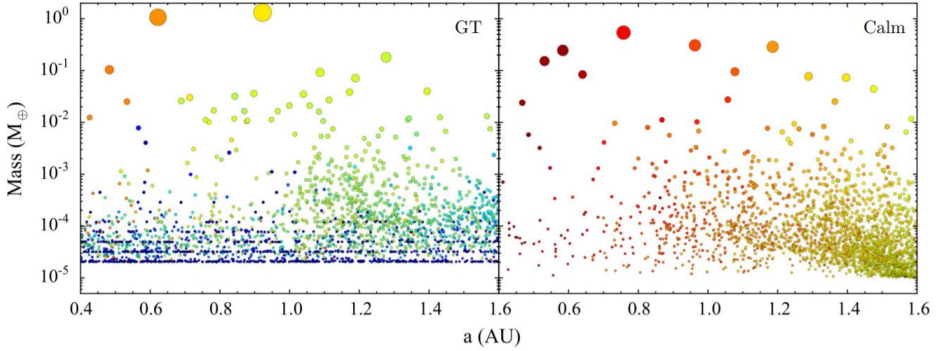
Figure 6.11: Two figures visualising the mass distribution of planetesimals grown from dynamic n-body simulations retrieved from [27]. The left hand panel visualises the planetesimals under influence of scattering from the Jupiter. The right hand panel visualises the a calm scenario in which only planetesimal accretion took place among planetesimals. Each dot represents a planetesimal and the size of the dot represents the mass of the planetesimal and the simulation was ran up until a time of 6×10^5 years.

Grand Tack scenario, while the right panel visualises a calm scenario without influence of giant planets. The Grand Tack scenario was able to product Earth sized planets near 1AU. The calm scenario is not able to produce sized planets.

What this means for the model in this thesis, if the Grand Tack scenario would be incorporated, it would result in an increase in surface density of pebbles for the inner regions. Particles from outer regions would be relocated in the inner regions if scattering from the giant planets were simulated. An increase in surface density in the inner regions allows for the planets to grow.

6.6.3. TAPERED DISKS

From the results of section 6.3.3, the ice giants were also able to grew into a few hundred Earth sizes. This is most likely due to the available material in the outer regions of the PPD. If tapering were to be used, the gas surface density would take on the form [28]:

$$\Sigma_{gas}(r) = \Sigma_0 \left(\frac{r}{r_0} \right)^{-\gamma} exp \left[\left(-\frac{r}{r_{tap}} \right)^{2-\gamma} \right] \qquad (6.12)$$

Where r_{tap} is the radial distance at which the taper initiates, and γ is the power index. If a taper would be applied at r_{tap}, the densities would decrease at radii larger than r_{tap}. This would result in less pebbles in that region. If the radial distances of Uranus and Neptune would fall in that region, their growth would be decreased as less material is available and their masses would not be as large as in the simulations. In figure 6.12, a difference in gas surface density is given. This figure plots the tapered surface density if r_{tap} is set to be 15AU.

At 30AU, the location of Neptune, the tapered surface density is only 13% of the surface density without taper. This means that there is less material for the outer planets to grow which results in less massive planets. At 50AU, the tapered surface density is about
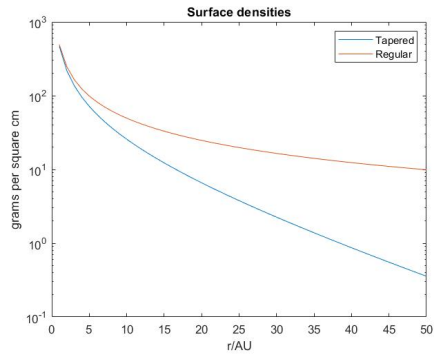
Figure 6.12: Two gas densities. The orange line represents the gas density used in this theses which includes a radial decay and the blue line represents a radial gas decay using incorporating tapering following equation 6.12.

4% of surface density without taper and this means that there will also be less incoming materials for planets at 30AU to grow from.

6

CONCLUSIONS

With the last chapter, all research questions in the introduction were investigated. The main research question was: *How are planets formed by pebble accretion?*

Chapter 3 addressed the formation of the pebbles. Within this chapter, the theory of settling and growth of ISM particles into sub-millimetre particles are addressed. However, it was highlighted that a specific radius does not mean that the particle is a pebble. This is when the definition by C. Ormel [3] gave clarity on what and what are not pebbles. Pebbles are particles with Stokes numbers of $10^{-3} < \tau_s < 1$. It was found in chapter 4 that settling and coagulations of particles resulted in little pebbles as the growth of particles from micron sized was not efficient. Particles ended up with small Stokes numbers, smaller than 10^{-3}. For this reason, two other growth scenarios were explored. One situation where there was gas decay, and another where turbulent motions were in play. The gas decay model did result in larger particles. However, it was also found that the Stokes numbers were reliant on the gas itself. As the gas decayed, the Stokes numbers of the particles increased and reached orders of 10^6 and thus, there were no pebbles. The turbulent model allowed for more growth of the particles and larger particles were found. These were suitable to be pebbles.

Using the build particles, a surface density was constructed of particles which were subjected to radial drift in chapter 5. The radial drift of particles result in changes in mass distribution over the disk over a period of time. The surface density changes and the changes were followed. This way, surface densities of both the particles and the pebbles among the particles, over time was constructed.

In chapter 6, the pebble accretion process to grow a core to a planet sized body is investigated. The input for the pebble accretion is the pebble surface densities over time. Assuming a planet core to be present, it would gain mass by accreting only the pebbles via pebble accretion. This way, planets are formed using pebble accretion. The simulation was performed for both the standard scenario and the turbulent scenario and planets were formed from the turbulent scenario. The planets formed were positioned at the locations of Earth, Jupiter, Saturn, Uranus and Neptune. The planet at the location of Earth was not able to grow, but all other planets did grow. The planet at Saturns location reached 100 Earth sizes and all other planets reached about 60 Earth sizes. It was found that the planets in the outer regions were able to grow efficiently as more pebbles were present in the outer region.

6.7. RECOMMENDATIONS

The following recommendations are given:

- Perform the settling with growth using multiple growth sources as opposed to one growth source. In this thesis, only one growth source was used during settlement. Multiple growth sources are present such as Brownian growth, settling growth and

turbulent growth. However during the simulations, only the largest source was used for growth while the growth should be a combination of all effects;

- Perform the gas decay model with different disk lifetime parameter τ_{disk}. In this thesis, two disk lifetimes were used: $\tau_{disk} = 10^6$ years and $\tau_{disk} = 500$ years. The former disk lifetime showed little effect for the settling process as settling took place in a shorter timescale. τ_{disk} did show differences during settling, but the gas decayed too rapidly. This resulted in no radial of the particles and no pebbles;

- Perform radial drift where the particles are able to grow. In this thesis, the radial drift was simplified by omitting the growth of particles during radial drift. Particles are able to grow as radial drift allows for collisions among particles;

- Test the pebble accretion theory with help of a different chemical model. Observations via a chemistry model can verify the pebble accretion theory;

- Include effects of Grand Tack scenario. In Grand Tack, Jupiter and Saturn migrate inwards and outwards. During this voyage, particles and planetesimals are scattered and the inner region receive these planetesimals from the outer regions. This favours the growth of planets in the inner region and the Earth would grow into a larger size;

- Include a gas exponential model with disk tapering into consideration. Disk tapering encapsulates the smoothing of outer edges of PPDs. This reduces the amount of material available for the outer planets to grow from, resulting in planets more in line with the actual outer planets.

A

APPENDIX - SETTLING VALIDATION

In this appendix, validation is given on the settling model. Chapter 4 models the settlement of particles towards the midplane and during settling, the particle is able to grow due to collisions with other smaller particles, and also grow from the dust density. Furthermore, three variations of the models are performed: one standard model with only growth from dust and particles, a gas decay model where the gas decreases over time as well, and a turbulent model which induces relative turbulent velocities for larger growth.

A.1. GROWTH

The growth of a particle from dust and collisions between another particle is given as:

$$\frac{dm}{dt} = \frac{dm}{dt}_{dust} + \frac{dm}{dt}_{particle} = \pi a^2 \left(v_{settle}\rho_d + \Delta v \rho_{particle} \right)$$

Where a is the radius of the particle, v_{settle} is the settling velocity, Δv is the relative velocity between the particle and other collision particle, ρ_d is the dust density and $\rho_{particle}$ is the particle density of the collision particle.
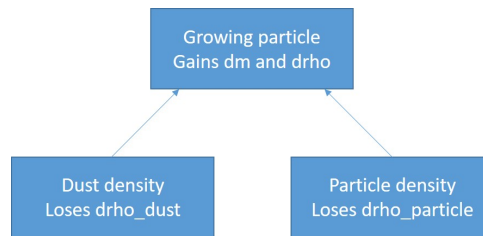
Figure A.1: Cartoon visualising the transfer of density from dust and particle to larger particle.

The decrease in dust density is due to the growth of the particle is:

$$\frac{d\rho_{dust}}{dt} = \frac{dm}{dt}_{dust} \cdot n$$

71

Where n is the number density of the particle growing from the dust. The growth of particle density of the growing particle is:

$$\frac{d\rho_{particle}}{dt} = \frac{dm}{dt}_{particle} \cdot n$$

$\frac{d\rho_{particle}}{dt}$ is also the decrease in particle density of the particle which is being fed to the larger growing particle.

A.2. SIMULATION

The grid of the program is spaced in time and and height above the midplane. The height is spaced in steps of $dz = 0.01h$ from 0 to $4h$ and each particle is initially positioned between a dz. For 0 to $4h$, this would mean that there are a total of 401 particles, $z = 0$ included. As the particles settle, they lose height according to the settling speed:

$$\frac{dz}{dt} = \frac{\Omega^2 \rho_{material} a z}{\bar{v} \rho_{gas}}$$

Where $\rho_{material}$ is the material density of the particle, and $\bar{v}$ is the mean thermal velocity.

As the simulation starts, particle settle, grow using the Euler forward method. Dust densities decrease as they are eaten by particles. The timestep between each step is set at 0.01 years and the program is ran for a time. If the final time is set to 1000 years, matrices result with dimensions of $(i, j) = 100000 \times 401$. These could for instance be the vertical height matrix, which describes the vertical position for each time (i) and each particle (j) or the radius matrix of the particle, which describes the radius per time (i) per particle (j).

The dust density matrix also has dimensions of $(i, j) = 100000 \times 401$ and described the dust density at time i and at which altitude above the midplane (j).

A.3. TIMESTEP

AS stated in the previous section, a timestep dt is chosen to be 0.01year. The simulation evolves parameters which are intertwined and dependent on each other. For instance, growth of a particle dm is dependent on the particle density of the encountered particle $\rho_{particle}$. Which in itself is another growing parameter. If dt were larger, the decrease in density for the dust density $\frac{d\rho_{dust}}{dt}$ or $\frac{d\rho_{particle}}{dt}$ might be larger than the actual dust density ρ_d or particle density $\rho_{particle}$:

$$\rho_{d_{i+1}} = \rho_{d_i} - \frac{d\rho_d}{dt} \cdot dt < 0 \ \ or \ \ \rho_{particle_{i+1}} = \rho_{particle_i} - \frac{d\rho_{particle}}{dt} \cdot dt$$

Furthermore, if dt were to made smaller, it was found that there was little settling after some years. For efficiency and computation time, $dt = 0.01$ years was used.

A.4. Conservation of Mass

From the equations in section 1, it can be traced that the growth of particle is dependent on the dust and other smaller particles. Furthermore, the growth of smaller particles is also dependent on the dust and other smaller particles. This means that the growth of all particles is only dependent on the dust and the mass of the dust is converted into particle mass. The total mass of particles cannot exceed the initial available mass from the dust. The conservation is visualised in figure A.2 where the evolution of the total density of dust and particles are visualised.
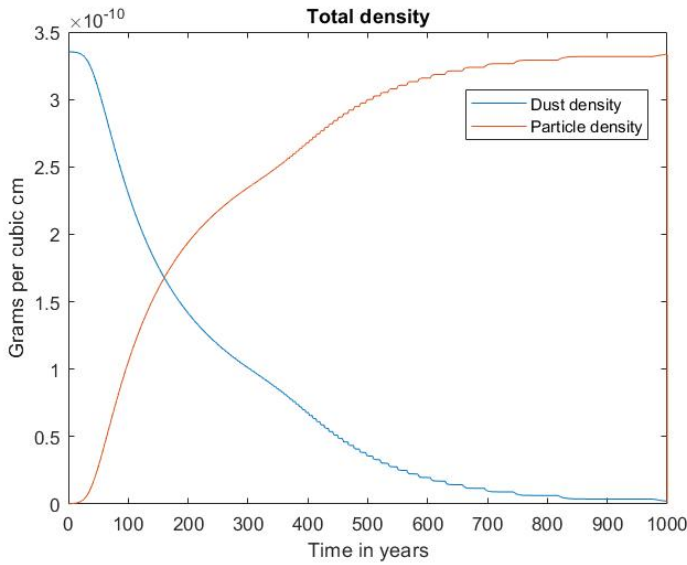
Figure A.2: The conversion of the total dust density into particle density. The blue line represents the total dust density and the orange line represents the total particle density. As the particles grow from the dust (and each other) dust density is transfered into the total particle density. This means that the exact decrease in total dust density has to be the total growth in particle density, which is visualised in this figure.

REFERENCES

[1] L. I. Cleeves, K. I. Öberg, D. J. Wilner, J. Huang, R. A. Loomis, S. M. Andrews, and I. Czekala, *THE COUPLED PHYSICAL STRUCTURE OF GAS AND DUST IN THE IM lup PROTOPLANETARY DISK,* The Astrophysical Journal **832,** 110 (2016).

[2] T. Montmerle, J.-C. Augereau, M. Chaussidon, M. Gounelle, B. Marty, and A. Morbidelli, *3. solar system formation and early evolution: the first 100 million years,* Earth, Moon, and Planets **98,** 39 (2006).

[3] C. W. Ormel, *The Emerging Paradigm of Pebble Accretion,* in *Formation, Evolution, and Dynamics of Young Solar Systems, Astrophysics and Space Science Library, Volume 445. ISBN 978-3-319-60608-8. Springer International Publishing AG, 2017, p. 197,* Astrophysics and Space Science Library, Vol. 445, edited by M. Pessah and O. Gressel (2017) p. 197.

[4] P. J. Armitage, *Lecture notes on the formation and early evolution of planetary systems,* arXiv e-prints (2007).

[5] L. Hartmann, *Accretion processes in star formation,* Vol. 32 (Cambridge University Press, 2000).

[6] F. LeBlanc, *An introduction to stellar astrophysics* (John Wiley & Sons, 2011).

[7] J. Blum and G. Wurm, *The growth mechanisms of macroscopic bodies in protoplanetary disks.* **46,** 21 (2008).

[8] S. J. Weidenschilling, *Dust to planetesimals: Settling and coagulation in the solar nebula,* **44,** 172 (1980).

[9] Y. Alibert, C. Mordasini, W. Benz, and C. Winisdoerffer, *Models of giant planet formation with migration and disc evolution,* **434,** 343 (2005), arXiv:astro-ph/0412444 [astro-ph] .

[10] H. Tanaka, T. Takeuchi, and W. R. Ward, *Three-dimensional interaction between a planet and an isothermal gaseous disk. i. corotation and lindblad torques and planet migration,* **565,** 1257 (2002).

[11] W. R. Ward, *Protoplanet Migration by Nebula Tides,* **126,** 261 (1997).

[12] T. Birnstiel, *The Evolution of Gas and Dust in Protoplanetary Accretion Disks,* Ph.D. thesis, - (2011).

[13] C. P. Dullemond and C. Dominik, *Dust coagulation in protoplanetary disks: A rapid depletion of small grains,* **434,** 971 (2005).

[14] C. Hayashi, *Structure of the Solar Nebula, Growth and Decay of Magnetic Fields and Effects of Magnetic and Turbulent Viscosities on the Nebula,* Progress of Theoretical Physics Supplement **70,** 35 (1981).

[15] S. J. Weidenschilling, *Aerodynamics of solid bodies in the solar nebula.* **180**, 57 (1977).

[16] M. Lambrechts and A. Johansen, *Forming the cores of giant planets from the radial pebble flux in protoplanetary discs,* **572**, A107 (2014).

[17] E. E. Mamajek, *Initial conditions of planet formation: Lifetimes of primordial disks,* AIP Conference Proceedings **1158**, 3 (2009), https://aip.scitation.org/doi/pdf/10.1063/1.3215910 .

[18] D. McNeil, M. Duncan, and H. F. Levison, *Effects of Type I Migration on Terrestrial Planet Formation,* **130**, 2884 (2005).

[19] H. Nomura and Y. Nakagawa, *Dust size growth and settling in a protoplanetary disk,* The Astrophysical Journal **640**, 1099 (2006).

[20] Y. Nakagawa, M. Sekiya, and C. Hayashi, *Settling and growth of dust particles in a laminar phase of a low-mass solar nebula,* **67**, 375 (1986).

[21] T. Takeuchi and D. N. C. Lin, *Radial Flow of Dust Particles in Accretion Disks,* **581**, 1344 (2002).

[22] C. W. Ormel and H. H. Klahr, *The effect of gas drag on the growth of protoplanets. Analytical expressions for the accretion of small bodies in laminar disks,* **520**, A43 (2010).

[23] J. Binney and S. Tremaine, *Galactic dynamics* (1987).

[24] A. Johansen and M. Lambrechts, *Forming planets via pebble accretion,* Annual Review of Earth and Planetary Sciences **45**, 359 (2017).

[25] M. Lambrechts and A. Johansen, *Rapid growth of gas-giant cores by pebble accretion,* Astronomy and Astrophysics **544**, A32 (2012).

[26] A. Pierens, S. N. Raymond, K. Walsh, E. Bolmont, and C. Cossou, *Inward-then-outward migration of Jupiter and Saturn and its implications for Uranus and Neptune, EPSC-DPS Joint Meeting 2011,* **2011**, 841 (2011), provided by the SAO/NASA Astrophysics Data System.

[27] P. J. Carter, Z. M. Leinhardt, T. Elliott, M. J. Walter, and S. T. Stewart, *Compositional Evolution during Rocky Protoplanet Accretion,* **813**, 72 (2015).

[28] T. Birnstiel and S. Andrews, *On the outer edges of protoplanetary dust disks,* The Astrophysical Journal **780** (2013), 10.1088/0004-637X/780/2/153.